SEDIMENTARY ENVIRONMENT AND DEPOSITIONAL SEQUENCES OF THE QOM BASIN (NORTH-EASTERN MARGIN OF THE TETHYAN SEAWAY)

Tayyeb BINAZADEH, **Amrollah SAFARI** * & **Hossein VAZIRI-MOGHADDAM**

Department of Geology, University of Isfahan, P.O.Box: 81746-73441 Isfahan, Iran;
e-mails: Tayyeb.binazadeh@yahoo.com, safari@sci.ui.ac.ir,
a.safari901@gmail.com, avaziri7304@gmail.com
* *Corresponding author*

Abstract: This research attempted to determine the depositional sequences of the Qom Formation in the Urumieh-Dokhtar arc (Ghamsar section) and Esfahan-Sirjan fore-arc (Abadeh section) sub-basins in Iran, using microfacies and microtaphofacies analyses. The authors also investigated connections between the Qom Basin and the Zagros and Paratethys basins during the Oligocene. In this regard a total of eight microfacies, two terrigenous facies, and five microtaphofacies were identified on the basis of 269 samples from the Ghamsar section and 93 samples from the Abadeh section. The studied microfacies, terrigenous facies, and microtaphofacies were deposited on a homoclinal carbonate ramp. This carbonate platform can be divided into inner, middle and outer ramp environments. On the basis of the distribution of microfacies and sequence stratigraphy studies, five third-order depositional sequences and one incomplete depositional sequence were identified in the Ghamsar section and three third-order depositional sequences in the Abadeh section. According to the distribution of microtaphofacies and palaeo-bathymetric studies based on *Amphistegina*, the energy, and depth of the Qom sea in the Ghamsar section were greater than those evidenced in the Abadeh section. The results of local fault activity in the different sub-basins of the studied sections indicate a lesser effect of global sea-level changes in the Paratethys basin. On the basis of the formation of depositional sequences in these sub-basins; and differences in the number of depositional sequences; intense local fault activity is indicated during the Chattian Age (especially in the Urumieh-Dokhtar arc sub-basin). Regional sea-level fluctuations of the south Tethyan Seaway and the Paratethys Basin controlled sea-level changes in the Chattian Age. The depositional basins of the Tethyan seaway (southern Tethyan seaway, Paratethys Basin and Qom Basin) probably were related during the Burdigalian to Langhian and the early Serravallian. The results show that, the effect of sea-level changes of the Zagros Sea on the formation of depositional sequences in the Esfahan-Sirjan fore-arc sub-basin was significant.

Key words: Qom Formation, Ghamsar section, Abadeh section, local faults, Tethyan Seaway.

Manuscript received 29 November 2022, accepted 20 February 2024

INTRODUCTION

The Iranian plateau contains the Zagros, Sanandaj-Sirjan, Urumieh-Dokhtar magmatic arc, Alborz, Central Iran, Lut, Kopeh Dagh, and Makran structural-sedimentary zones (Fig. 1b; Berberian and King, 1981; Heydari, 2008). The Central Iran zone is part of the Alpine-Himalayan orogenic system. This structural-sedimentary zone is surrounded by the Palaeotethys and Neotethys suture zones in the north and south, respectively (Nadimi, 2007). According to Berbarian (2005), the closure of the Neotethys and subduction of the oceanic crust beneath the continental crust of Central Iran led to the formation of the sedimentary basin of the Qom Formation (Berberian, 2005).

Harzhauser and Piller (2007) and Reuter *et al.* (2009) showed that the Qom sedimentary basin is located on the northern margin of the Neotethys basin. During the Oligocene, carbonate platforms dominated by coralline algae and benthic foraminifera developed along the margins of the Tethys Sea as well as in the Tethyan Seaway in the Iranian Plate and the Atlantic and Indo-Pacific realms (Bover-Arnal *et al.*, 2017). Microfacies analysis and

palaeoenvironmental interpretation of the Qom Formation show that Qom Formation was deposited in a variable depositional system (Mohammadi *et al.*, 2011).

According to Mohammadi and Ameri (2015), the study of the Oligo-Miocene deposits of Central Iran (Qom Formation) and reconstruction of their depositional environments are essential and important because of: (1) their economic importance, since the Qom Formation is the main target for oil and gas exploration in Central Iran (Morley *et al.*, 2009), and (2) at the same time, the Central Iran Sea had a communicative role between the Eastern Tethys (the proto-Indian Ocean) and the Western Tethys region (the proto-Mediterranean Sea).

The Qom basin has been divided according to many researchers into the Qom back-arc and Esfahan-Sirjan fore-arc sub-basins (Fig. 1a; Harzhauser and Piller, 2007; Reuter *et al.*, 2009). However, Mohammadi *et al.* (2013) added a third sub-basin (Urumieh-Dokhtar arc sub-basin) to the Qom basin (Fig. 1a). The connection between the Neotethys and Paratethys basins was established during the Oligocene–Miocene time (Harzhauser and Piller, 2007).

The connection between the Qom back-arc basin and the Paratethys basin is suggested to have been fully established from the Burdigalian Age onwards (Mahyad *et al.*, 2019; Safari *et al.*, 2020a, b). The objectives of this study are as follows:

1. Reconstruction of palaeoconditions of the Oligocene deposits (Qom Formation) of the Urumieh-Dokhtar arc and Esfahan-Sirjan fore-arc sub-basins of the Qom basin, based on microfacies and microtaphofacies.
2. Reconstruction of the sedimentary environment and depositional sequences in the study sections.
3. Investigation of the connection between the Urumieh-Dokhtar arc and Esfahan-Sirjan fore-arc sub-basins and the Zagros sedimentary basin (southern margin of Neotethys basin).

GEOLOGICAL SETTING AND PREVIOUS WORK

The Qom Formation in the Qom back-arc, Urumieh-Dokhtar arc, and Esfahan-Sirjan fore-arc sub-basins contains a thick sequence of gypsum, marl, limestone, and siliciclastic deposits (Stocklin and Setudehnia, 1991; Reuter *et al.*, 2009). The Oligo-Miocene deposits of the Central Iran zone were first divided into six members (A, B, C, D, E, and F; Furrer and Soder, 1955; Gansser, 1955). In addition, C was divided into four members (C1, C2, C4, and C5; Abaie *et al.*, 1964).

The Qom Formation overlies the Eocene volcanic rocks in the Ghamsar section and is covered by Recent alluvial sediments. The Qom Formation in the Ghamsar section is 313 m thick and is mostly composed of medium- and thick-bedded and massive limestones and shales. The lower section of the studied sequence in the Ghamsar section is 161 m thick. It consists of thick-bedded to massive limestones, while an alternation of medium-bedded limestones and shales with a thickness of 152 m forms the upper part of the studied section. The Qom Formation overlies the Lower Red Formation in the Abadeh section and is covered by the Recent alluvium. The Qom Formation, 164 m thick in the Abadeh section, is mostly composed of medium- and thick-bedded and massive limestones and shales. The lower part of the studied section is 117 m thick and consists of shales and medium- and thick-bedded limestones. Massive limestones (47 m thick) form the upper part of the studied sequence.

MATERIAL AND METHODS

In order to achieve the objectives of the study, two sections of the Oligocene succession (Qom Formation) in the
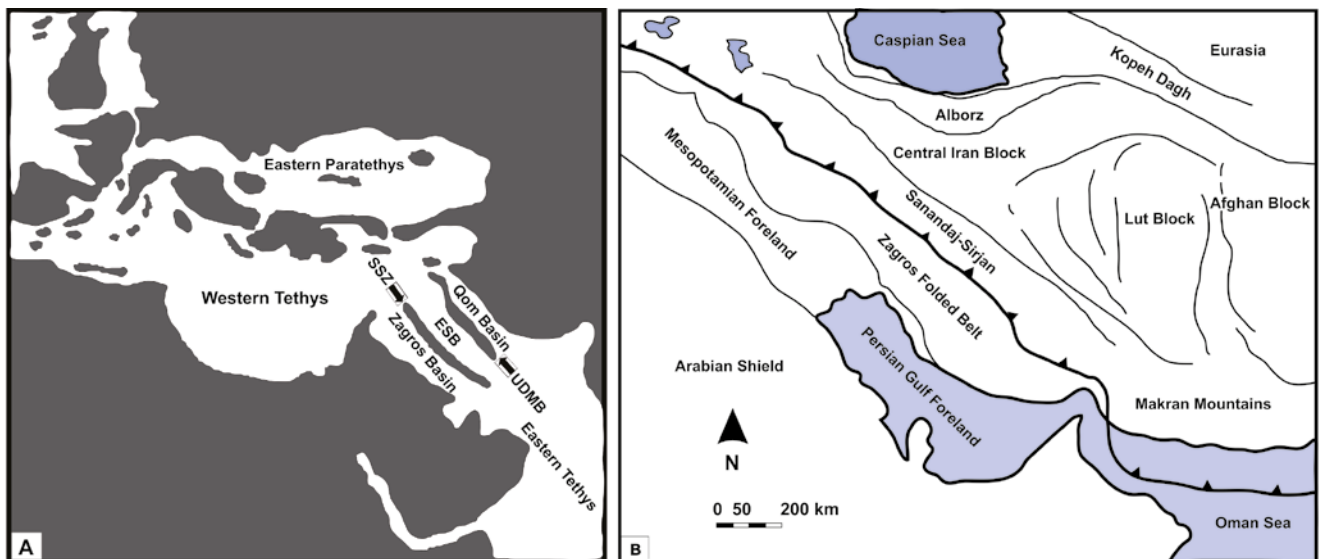
Fig. 1. Palaeobiogeographical and tectonic map. **A.** Palaeogeography of the Neotethys basins during the Oligocene Epoch. SSZ – Sanandaj-Sirjan zone; ESB – Esfahan-Sirjan sub-basin, UDMB – Urumieh-Dokhtar sub-basin (modified from Harzhauser and Piller, 2007 and Reuter *et al.,* 2009). **B.** Structural-sedimentary zones of the Iranian plateau (modified from Heydari *et al.,* 2003).

Urumieh-Dokhtar arc (Ghamsar section) and Esfahan-Sirjan fore-arc sub-basins (Abadeh section) were studied. The Ghamsar section (51°26′13′′ E, 33°46′45′′ N) is located 3km north of Ghamsar (south of Kashan). The Abadeh section (52° 43′59′′ E, N: 31°30′61′′ N) lies 40 km northeast of Abadeh (south of Isfahan) (Fig. 2).

A total of 252 (limestone) and 17 (shale) rock samples from the Ghamsar section and 81 (limestone) and 12 (shale) rock samples from the Abadeh section were collected. Thin sections were obtained from hard samples. Soft samples (shale) were washed with 10% hydrogen peroxide, then disaggregated by melting and freezing and then microfossils were isolated by hand-picking. Features, such as sediment texture, grain size and fossil content, were used to determine microfacies. The sedimentary texture of thin sections was determined, using the classifications of Dunham (1962), and Embry and Klovan (1971). Abundant large benthic foraminifera, corals, bryozoans, corallinaceae (red algae) in the Ghamsar and Abadeh sections were used to determine microtaphofacies.

The taphonomic signatures (fragmentation, abrasion, encrustation, and bioerosion) were evaluated on the basis of Allison and Bottjer (2011), Silvestri et al. (2011), Bover-Arnal et al. (2017). The qualitative classification presented by Beavington-Penney (2004), was used to evaluate the damage to large benthic foraminifera tests.

Previous studies, such as Brachert et al. (1998), Nebelsick and Bassi (2000), Allison and Bottjer (2011), Nebelsick et al. (2011) and Silvestri et al. (2011), were used to identify microtaphofacies. The thickness-to-diameter ratio of Amphistegina tests (T/D) changes with increasing seawater depth (Larsen and Drooger, 1977; Hallock and Hansen, 1979; Hallock and Glenn, 1986; Hallock, 1999; Mateu-Vicens et al., 2009). The T/D ratio was used to determine the depth of seawater under specific nutrient conditions (Mateu-Vicens et al., 2009). On the basis of the formula Zom = 2.046 T/D – 2.293, Mateu-Vicens et al. (2009) presented a diagram to determine the depth of seawater under oligo-mesotrophic nutrient conditions.

In this study, the diameter and thickness of the tests were measured for 186 samples of Amphistegina in the Ghamsar section and 47 samples in the Abadeh section to calculate the T/D ratio of the samples. These were interpreted as being the conditions of formation of the investigated deposits, thanks to the presence of benthic foraminifera (imperforate and perforate foraminifera), corals and corallinaceae in the studied sections, indicating oligo-mesotrophic nutrient conditions (Hottinger, 2000; Langer and Hottinger, 2000;
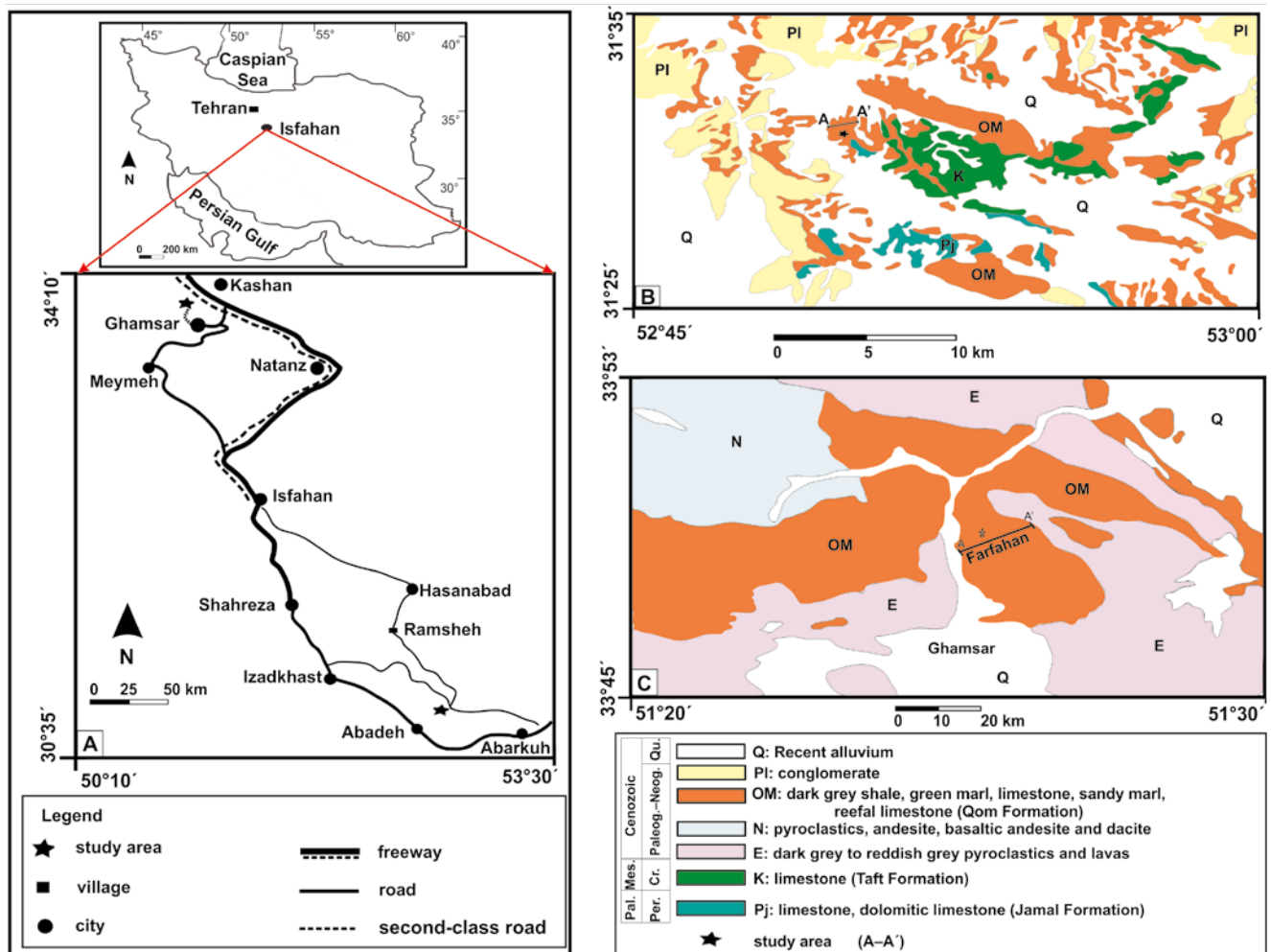
Fig. 2. Locality and geological map. **A.** Road map of the Ghamsar and Abadeh sections. **B.** Geological map of the Abadeh section (Taraz and Aghanabati, 1993). **C.** Geological map of the Kashan section (Amidi and Zahedi, 1991).

Halfar *et al.*, 2004; Payros *et al.*, 2010; Pomar *et al.*, 2014). As a result, the approximate palaeo-depth of seawater was determined for each of the microfacies, using a diagram introduced by Mateu-Vicens *et al.* (2009) and the sea-level change was plotted for both sequences studied.

RESULTS

Description of microfacies

The Qom Formation in the Ghamsar and Abadeh sections shows eight microfacies, based on the distribution of benthic foraminifera, other skeletal components and sedimentological features (Tab. 1).The main components of the sandy bioclast packstone-grainstone (MF 1) microfacies included miliolids, *Neorotalia*, *Elphidium*, corallinaceae, echinoderms, and terrigenous components (quartz grains; Fig. 3A). *Pseudolituonella*, *Dendritina*, *Triloculina*, *Textularia*, and bryozoans are sub-components. This microfacies was observed only in the Ghamsar section. The results of palaeoobathymetric studies, based upon the *Amphistegina* T/D ratio, show that microfacies 1 was deposited at a water depth of 11 m (Tab. 2).

Imperforate foraminifera (miliolids, *Quinqueloculina*, *Austrotrillina*, *Triloculina*, *Peneroplis*, *Borelis*, *Sorites* and *Dendritina*) and the corallinaceae are the main components of the microfacies of the bioclast corallinaceae imperforate foraminifera packstone-grainstone (MF 2; Fig. 3B). The subordinate components of the microfacies include coral fragments, gastropods, *Tubucellaria*, echinoids, valvulinids, bryozoans, and *Neorotalia*. In addition, coral fragments increase in some thin sections from the Qom Formation in the Ghamsar section. This microfacies was found in both study sections. In the Abadeh section, this microfacies developed at a water depth of 9 m (Tab. 3), while a water depth of approximately 12 m was estimated for the Ghamsar section (Tab. 2).

The imperforate foraminifera (*Austrotrillina*, *Quinqueloculina*, *Triloculina*, *Peneroplis*, miliolids, *Borelis*, and *Dendritina*), perforate foraminifera (*Neorotalia*, *Heterostegina*, *Lepidocyclina* and *Amphistegina*) and corallinaceae are abundant in the microfacies, consisting of bioclast corallinaceae imperforate and perforate foraminifera floatstone-packstone (MF 3; Fig. 3C). The subordinate components of the microfacies include corals, echinoids, gastropods and bivalve fragments, *Risananeiza*, *Planorbulina*, *Discorbis*, valvulinid, *Textularia*, *Sphaerogypsina*, *Tubucellaria* and ostracods. The microfacies was found in both of the study sections. This microfacies indicates a water depth of approximately 13 m and 14 m in the Ghamsar and Abadeh sections, respectively (Tabs 2, 3).

Table 1

Description and depositional environments of microfacies of the Qom Formation.

FM	Microfacies name	Main components	Location		Depositional environment
			Abadeh area	Ghamsar area	
MF 1	Sandy bioclast packstone-grainstone	Miliolids, *Neorotalia*, *Elphidium*, corallinaceae, echinoderms, quartz grains		*	Inner ramp
MF 2	Bioclast corallinaceae imperforate foraminifera packstone-grainstone	Imperforate foraminifera (miliolids, *Quinqueloculina*, *Austrotrillina*, *Triloculina*, *Peneroplis*, *Borelis*, *Sorites*, and *Dendritina*), corallinaceae	*	*	Inner ramp
MF 3	Bioclast corallinaceae imperforate and perforate foraminifera floatstone-packstone	Imperforate foraminifera (*Austrotrillina*, *Quinqueloculina*, *Triloculina*, *Peneroplis*, miliolids, *Borelis*, and *Dendritina*), perforate foraminifera (*Neorotalia*, *Heterostegina*, *Lepidocyclina* and *Amphistegina*), corallinaceae	*	*	Inner ramp
MF 4	Coral boundstone	Coral	*	*	Inner ramp/ middle ramp
MF 5	Bioclast coral corallinaceae packstone-floatstone	Corallinaceae, corals	*	*	Middle ramp
MF 6	Bioclast corallinaceae perforate foraminifera packstone-floatstone	Corallinaceae, perforate foraminifera (*Lepidocyclina*, nummulitids, *Neorotalia*, and *Amphistegina*)	*	*	Middle ramp
MF 7	Planktonic foraminifera bioclast packstone	Planktonic foraminifera, the fine fragments of large foraminifera		*	Outer ramp
MF 8	Bioclast planktonic foraminifera wackestone-packstone	Planktonic foraminifera		*	Outer ramp
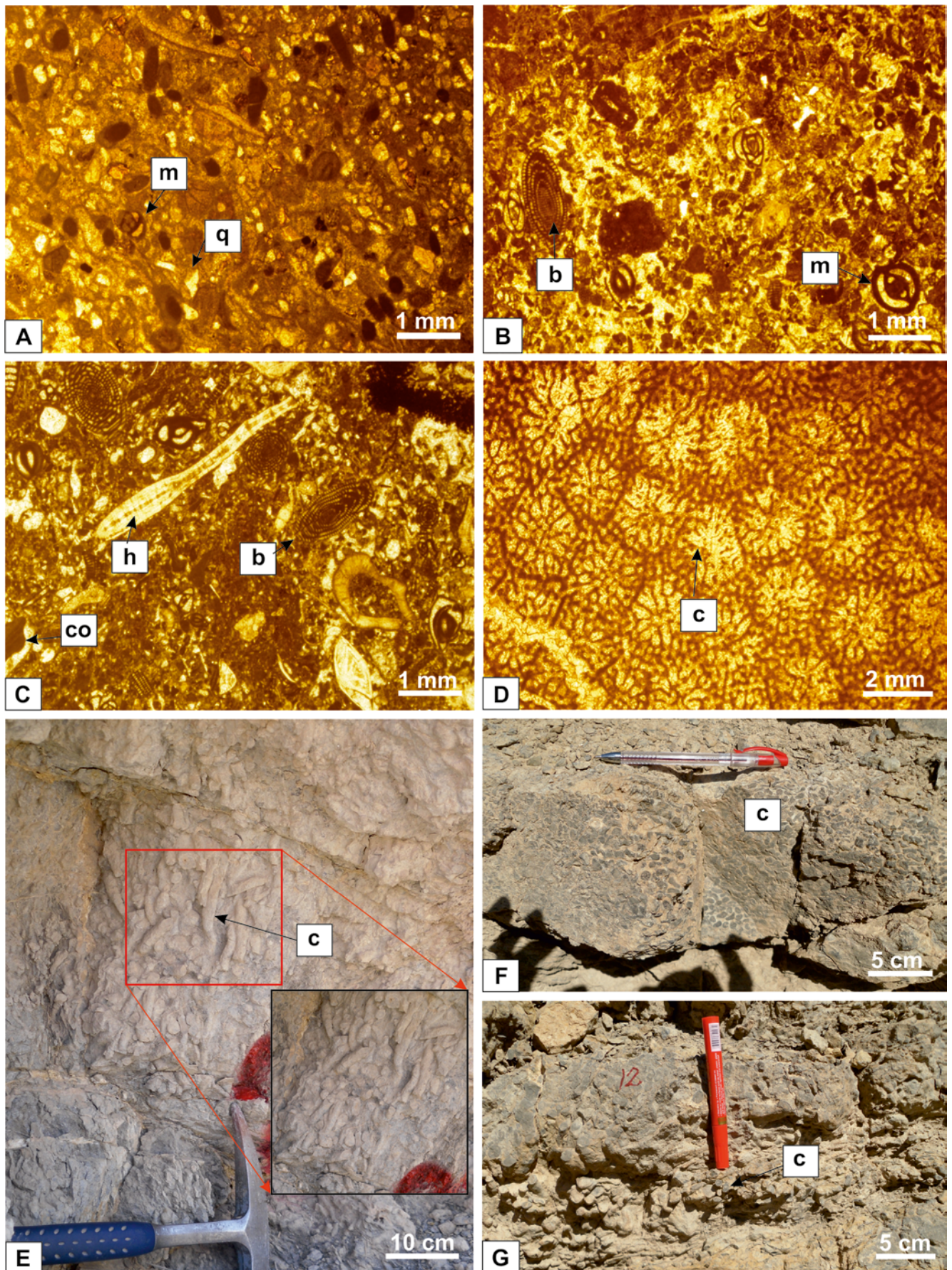
Fig. 3. Microfacies and field pictures. **A.** Sandy bioclast packstone-grainstone (MF 1); q – quartz grains; m – miliolids. **B.** Bioclast corallinaceae imperforate foraminifera packstone-grainstone (MF 2); m – miliolids; b – *Borelis*. **C.** Bioclast corallinaceae imperforate and perforate foraminifera floatstone-packstone (MF 3); h – *Heterostegina*; b – *Borelis*; co – Corallinaceae. **D.** Coral boundstone (MF 4); c – coral. **E–G.** Field photograph of the branching corals in the study sections.

Palaeodepth of sea based on *Amphistegina* T/D measurements in the Ghamsar section.

Microfacies	T (thickness; mm)	D (diameter; mm)	T/D (mm)	Depth of seawater (m)
MF 1	0/65	1/25	0/52	<11
MF 2	0/6	1/2	0/5	12
MF 3	0/6	1/25	0/48	13
MF 4	0/7	1/6	0/43	16
	0/65	1/6	0/4	19
MF 5	0/65	1/85	0/35	26
MF 6	0/7	2/1	0/33	29
MF 8	0/9	2/9	0/31	34
MF 9	0/6	2/1	0/28	44

Palaeodepth of sea based on *Amphistegina* T/D measurements in the Abadeh section.

Microfacies	T (thickness; mm)	D (diameter; mm)	T/D (mm)	Depth of seawater (m)
MF 1	-	-	-	-
MF 2	0.6	1.1	0.54	<9
MF 3	0.85	1.8	0.47	14
MF 4	0.7	1.6	0.43	16
MF 5	0.4	1	0.4	19
MF 6	0.5	1.65	0.3	36

Microfacies MF 4 consists of a coral boundstone (Fig. 3D). The framework of the microfacies is represented by intact corals that are found as scattered colonies and patch reefs in field observations. The microfacies included dome-shaped and branching corals in the Ghamsar section, but only dome-shaped corals were observed in the Abadeh section (Figs 3E, F, G, 4A, B). The branching corals appear in the lower layers of the Ghamsar section and then are replaced upwards by dome-shaped coral colonies, and finally branching corals predominate in the upper section of the studied sequence. Benthic foraminifera (such as miliolids, *Triloculina*, *Neorotalia*, and *Lepidocyclina*), corallinaceae, echinoderms and gastropods are subordinate components of microfacies 4.

The results of bathymetric studies based upon *Amphistegina* show that microfacies 4 in the Abadeh section was formed at a depth of approximately 16 m of seawater. In the Ghamsar section, colonies containing dome-shaped corals were formed at a depth of 16 m of seawater and branching coral colonies were formed at a depth of 19 m (Tabs 2, 3).

Corallinaceae and corals are major components of the bioclast coral corallinaceae packstone-floatstone microfacies (MF 5; Fig. 4C). Perforate foraminifera, such as *Neorotalia*, *Miogypsina*, *Lepidocyclina*, nummulitids, *Amphistegina*, *Elphidium*, and *Discorbis*, and imperforate foraminifera (e.g., miliolids, *Borelis*, *Planorbulina, Dendritina*, and *Meandropsina*) as well as echinoids, Valvulinids, *Textularia*,

Tubucellaria, and bryozoans are minor components of the microfacies. Microfacies 5 in the Ghamsar section developed at an approximate depth of 26 m and in the Abadeh section at an approximate depth of 19 m (Tabs 2, 3).

Corallinaceae and perforate foraminifera (*Lepidocyclina*, nummulitids, *Neorotalia*, and *Amphistegina*) are the main components of bioclast Corallinaceae perforate foraminifera packstone-floatstone (MF 6; Fig. 4D). Corals, *Elphidium*, echinoids, bryozoans, gastropods, *Quinqueloculina*, miliolids, *Austrotrillina*, *Textularia*, and *Discorbis* are subordinate components of this microfacies. Microfacies 6 in the Ghamsar section was deposited in a sea with an approximate depth of 29 m and in the Abadeh section in a sea with an approximate depth of 36 m (Tabs 2, 3).

Planktonic foraminifera and the fine fragments of large foraminifera are the main components of a planktonic foraminifera bioclast packstone (MF 7; Fig. 4E). The minor components of microfacies 7 include *Amphistegina*, *Textularia*, valvulinids, *Elphidium*, *Neorotalia*, *Discorbis*, *Ditrupa*, bryozoans, and bivalves. MF 7 in the Ghamsar section was formed in a sea approximately 34 m deep (Tab. 2).

Planktonic foraminifera are the main components of a bioclast planktonic foraminifera wackestone-packstone (MF 8; Fig. 4F). The minor components of MF 8 include small benthic foraminifera (such as Textularids), ostracods, *Elphidium*, *Planorbulina*, *Neorotalia*, *Discorbis*, bivalves, and corallinaceae. MF 8 in the Ghamsar section was deposited in a sea approximately 44 m deep (Tab. 2).
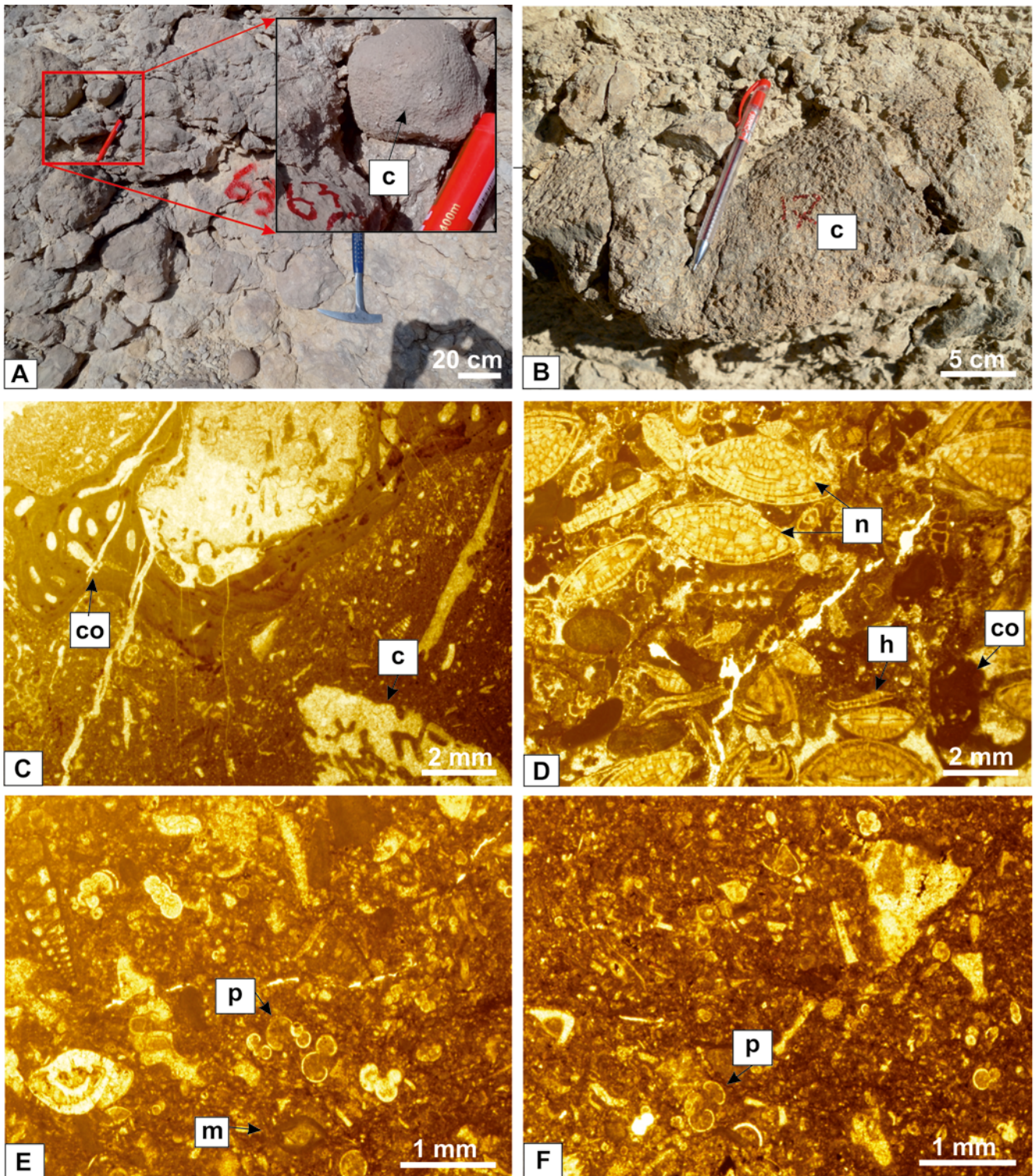
Fig. 4. Field and microfacies pictures. **A–B**. Dome-shaped l corals. **C.** Bioclast coral corallinaceae packstone-float-stone (MF 5); c – coral; co – Corallinaceae. **D.** Bioclast corallinaceae perforate foraminifera packstone-floatstone (MF 6); co – Corallinaceae; n – *Nummulites*; h – *Heterostegina*. **E.** Planktonic foraminifera bioclast packstone (MF 7); p – planktonic foraminifera; m – debris of miliolids. **F.** Bioclast planktonic foraminifera wackestone-packstone (MF 8); p – planktonic foraminifera.

According to the calcimetric test, the amount of lime in the sample of terrigenous facies was less than 10% and terrigenous particles in the size range of silt and clay were more than 90%. Also, according to the Walther's law, this terrigenous facies in the Abadeh section is in middle ramp (after MF 6) and contains perforate foraminifera (*Elphidium, Amphistegina*, small *Rotalia* and planktonic foraminifera). In the Ghamsar section, this terrigenous facies contains imperfo-rate foraminifera (miliolids and *Borelis*), and bryozoans, and alternates with the inner ramp microfacies (MF 2 and MF 4).

Description of microtaphofacies

Five microtaphofacies were identified on the basis of their main components and taphonomic signatures, such as fragmentation, bio-erosion, encrustation, disarticulation, and abrasion in the Ghamsar and Abadeh sections.

The main components of the first microtaphofacies (MTF 1) are corallinaceae, corals, and large imperforate foraminifera (*Borelis*, *Peneroplis*, *Sorites*, miliolids, *Dendritina*, and *Archaias*, Tab. 4; Fig. 5A). In the Abadeh section, taphonomic signatures, such as fragmentation and abrasion were high in the first microtaphofacies. However, in the Ghamsar section, the rate of fragmentation and abrasion was moderate to high. Encrustation and bio-erosion are absent in the first microtaphofacies. But in the Ghamsar section, bio-erosion and fragmentation were low and low to moderate, respectively.

Large perforate foraminifera (miogypsinid, *Heterostegina*, *Amphistegina* and *Neorotalia*), large imperforate foraminifera (*Archaias*, *Peneroplis*, *Penarchaias*, *Borelis* and *Sorites*), corals, corallinaceae and bryozoans are the components of the second microtaphofacies (MTF 2; Tab. 4; Fig. 5B). In the Abadeh section, the rate of fragmentation, disarticulation and abrasion in the second microtaphofacies is low to high. However, fragmentation and abrasion are variable from moderate to high rates in the Ghamsar section. The rate of encrustation in both study sections is low to moderate. The rate of bio-erosion is low to moderate in the Abadeh section, but low in the Ghamsar section.

Corals are the major components of the third microtaphofacies (MTF 3; Tab. 4; Fig. 5C). In the Abadeh and Ghamsar sections, the rate of fragmentation and abrasion in the third microtaphofasis is low to moderate. Encrustation is absent in the Abadeh section; however, the rate of encrustation in Ghamsar section is low to moderate. The bio-erosion of the third microtaphofacies is low in the Abadeh and Ghamsar sections.

The fourth microtaphofacies (MTF 4) consists of debris of corallinaceae and corals (Tab. 4; Fig. 5D). The rate of fragmentation and abrasion in the fourth microtaphofacies is low to moderate in the Abadeh section, and low to high in the Ghamsar section. The rate of encrustation in the Abadeh

Table 4

Description of microtaphofacies in the study sections (microtaphofacies: MTF; A – Abadeh section; G – Ghamsar section).

MTF names	Major components	Fragmentation/ disarticulation				Abrasion				Bioerosion			Encrustation			Abrasion of large benthic foraminifera (category)		
		L-M	L-H	M-H	H	L-M	L-H	M-H	H	No	L	L-M	NO	L-M	L-H	NO	1-3	2-3
MTF 1	Corallinaceae red algae, corals, and imperforate large benthic foraminifera (*Borelis*, *Peneroplis*, *Archaias*, *Dendritina*, *Sorites*, and miliolids)	-	-	GH	A	-	-	GH	A	A	GH	-	A	GH	-			GH and A
MTF 2	Imperforate foraminifera (*Borelis*, *Peneroplis*, *Archaias*, *Sorites*, and *Penarchaias*), perforate foraminifera (*Amphistegina*, *Neorotalia*, and *Heterostegina*), Corallinaceae red algae, corals, and bryozoans	-	A	GH	-	-	A	GH	-	-	GH	A	-	GH and A	-	-	-	GH and A
MTF 3	Corals	GH and A	-	-	-	GH and A	-	-	-	-	GH and A	-	A	GH	-	GH and A	-	-
MTF 4	Corallinaceae red algae, corals	A	GH	-	-	A	GH	-	-	-	-	GH and A	-	-	GH and A	GH and A	-	-
MTF 5	Large perforate foraminifera (*Amphistegina*, *Neorotalia*, *Heterostegina*, *Operculina*, and *Lepidocyclina*), Corallinaceae red algae, corals, bryozoans, and planktonic foraminifera	-	-	GH and A	-	-	-	GH and A	-	-	GH	A	-	GH and A	-	-	A	GH

and Ghamsar sections is estimated as low to high. The multilayer encrustation was observed around different types of skeletal grains in the Abadeh section and especially in the Ghamsar section. In the fourth microtaphofacies, bio-erosion was low to moderate in the Abadeh and Ghamsar sections.

Imperforate foraminifera (*Lepidocyclina*, *Heterostegina*, *Amphistegina*, *Neorotalia*, *Operculina*, and miogypsinid), planktonic foraminifera, corals, bryozoans, and corallinaceae are the main components of microtaphofacies MTF 5 (Tab. 4; Fig. 5E, F). The taphonomic signatures, such as fragmentation and abrasion, of microtaphofacies MTF 5 in
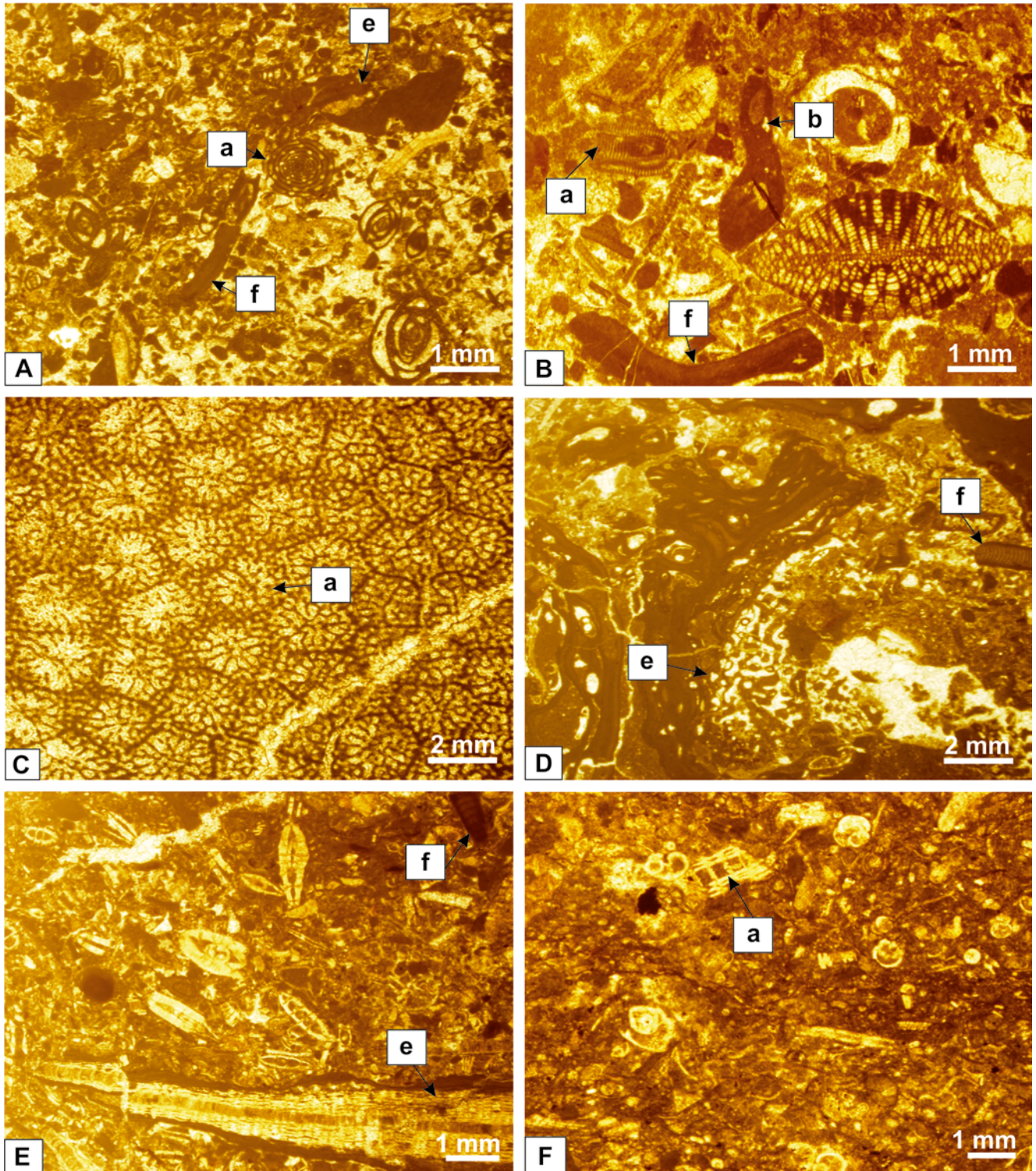
Fig. 5. Microtaphofacies pictures. **A.** First microtaphofacies (MTF 1); a – abrasion of large benthic foraminifera; e – encrustation; f – fragmentation. **B.** Second microtaphofacies (MTF 2); a – abrasion of large benthic foraminifera; b – bio-erosion; F – fragmentation. **C.** Third microtaphofacies (MTF 3); a – abrasion. **D.** Fourth microtaphofacies (MTF 4); e – encrustation; f – fragmentation. **E–F.** Fifth microtaphofacies (MTF 5); e – encrustation; f – fragmentation; a – abrasion of large benthic foraminifera.

the Abadeh and Ghamsar sections have moderate to high rates. Encrustation in the Abadeh and Ghamsar sections shows a low to moderate rate. Bio-erosion indicates in the Abadeh and Ghamsar sections low to moderate and low rates, respectively.

DISCUSSION

Sedimentary environments

Reefal, oolitic and bioclastic barriers were abundant in carbonate ramps (Read, 1982, 1985; Buxton and Pedly, 1989; Flügel, 2010). The facies of the reef barrier and other barriers (e.g., skeletal and ooid) are absent in the sediments of the Qom Formation in the Ghamsar and Abadeh sections.

According to the above findings, the sediments of the Qom Formation in the Ghamsar and Abadeh sections were deposited in a homoclinal carbonate ramp. (Figs 6, 7, 8). This carbonate platform contained the inner, middle and outer ramp environments. The presence of quartz grains along with skeletal allochems (miliolids and gastropods) in carbonate sediments indicates that these sediments were formed in normal marine shallow water and influenced by continental runoff and along coastal currents that brought sand (Geel, 2000; Brandano *et al.*, 2010; Pomar *et al.*, 2014). Therefore, a sandy bioclastic packstone-grainstone (MF 1) was formed in the inner ramp. MF 1 was absent in the Abadeh section and in the Ghamsar section MF 1 developed at a depth of 11 m.

The association of imperforate foraminifera with corallinaceae (red algae) indicates a high-energy environment with seagrass meadows (Pomar, 2001; Pomar *et al.*, 2017). In addition, the abundance of imperforate and perforate foraminifera as well as corallinaceae indicate an inner ramp with seagrass meadows (Pomar, 2001; Romero *et al.*, 2002; Beavington-Penney *et al.*, 2006; Afzal *et al.*, 2011; Nebelsick *et al.*, 2013). Therefore, the bioclastic corallinaceae imperforate foraminifera packstone-grainstone (MF 2) and bioclast corallinaceae imperforate and perforate foraminifera floatstone-packstone (MF 3) were deposited in a normal marine shallow water environment with seagrass meadows.

The coral boundstone (MF 4) was formed at the limit between the inner and middle ramp, just a few metres deeper than the seagrass. The MF 4 (less than 9–16 m depth) in the Abadeh section was shallower than the MF 4 (depth of 11–19 m) in the Ghamsar section. Moreover, Yazdi *et al.* (2012) showed that thin branching corals lived in a deeper environment than that of dome-shaped and massive corals. In fact, the deeper marine environment in the Ghamsar section provided suitable conditions for the growth of branching coral colonies. However, in the Abadeh section colonies of dome-shaped corals are abundant, owing to the shallower depth of the marine environment. This is consistent with the results of palaeobathymetric studies, based upon *Amphistegina,* in the study sections. In addition, dome-shaped and branching coral colonies are seen alternately in the Ghamsar section. In fact, in the Ghamsar section, branching coral colonies first appeared with increasing seawater depth and then with decreasing water depth, dome-shaped coral colonies predominated and finally branching coral colonies occurred

with increasing seawater depth in the upper section of the sequence and replaced the dome-shaped corals. This indicates a change in environmental conditions (with increasing depth of seawater) for the upper section of the sequence studied in the Ghamsar section.

Owing to the similarity of the main components between the first, second, and third microtaphofacies and MFs 1, 2, and 3, it can be concluded that these microtaphofacies were formed in an inner ramp environment. The rate of fragmentation is directly related to the wave base and the depth of seawater, and the highest rate of fragmentation occurs in a high-energy environment (Nebelsick *et al.*, 2011). The moderate rate of fragmentation indicates a low- to high-energy depositional environment (Nebelsick *et al.*, 2011). The moderate rate of damage (category 2) to a high rate of damage (category 3) of the large benthic foraminiferal tests indicates more transport by waves or destruction of the tests by destructive fish and other organisms (Beavington-Penney, 2004). Encrustation occurs in a high-energy environment (Perry, 2005).

According to the above and the rates of taphonomic signatures in the studied sections, it can be concluded that the inner ramp in the Abadeh section reflects higher-energy conditions than that in the Ghamsar section.

The abundance of coral and corallinaceae indicates the middle ramp environment, below the fair-weather wave base, and mesophotic to oligophotic conditions (Pomar, 2001; Flügel, 2010; Pomar *et al.*, 2017; Sarkar, 2017).

Bioclastic coral corallinaceae packstone-floatstone (MF 5) was formed in the middle ramp environment. The fourth microtaphofacies had the same main components as MF 5 and was formed in the middle ramp environment. At a depth of 20 m of seawater, the rate of encrustation reaches its maximum level (Greenstein and Pandolfi, 2003). In the high-energy environments, the rate of encrustation is high (Silvestri *et al.*, 2011; Ćosović *et al.*, 2012; Bover-Arnal *et al.*, 2017). In a low- to high-energy environment, fragmentation varies from low to moderate (Silvestri *et al.*, 2011). The encrustation by bryozoans indicates a moderate- to high-energy environment (Berning *et al.*, 2009). MF 5 and microtaphofacies 4 were deposited at a greater depth in the Ghamsar section than in the Abadeh section. On the basis of the rate of allochem fragmentation and abrasion, the hydrodynamic energy of the Ghamsar section was greater than that of the Abadeh section.

However, multilayer encrustation by the corallinaceae and bryozoans indicates high energy as well as changes in environmental conditions (in terms of the influx of siliciclastics) in both sections. Large benthic foraminifera (*Heterostegina*, *Nummulites*, *Amphistegina*, and *Operculina*), *Neorotalia*, and red algae (Corallinaceae) are abundant in the proximal middle ramp environment and indicate mesophotic to oligophotic conditions (Brandano *et al.*, 2009, 2012; Quaranta *et al.*, 2012; Pomar *et al.*, 2014; Brandano *et al.*, 2016; Sarkar, 2017).

Bioclastic corallinaceae perforate foraminifera packstone-floatstone (MF 6) was deposited in the middle ramp environment and in mesophotic to oligophotic conditions. The abundance of planktonic foraminifera increases in open marine conditions and towards the deep part of the basin (Geel, 2000; Knoerich and Mutti, 2003).
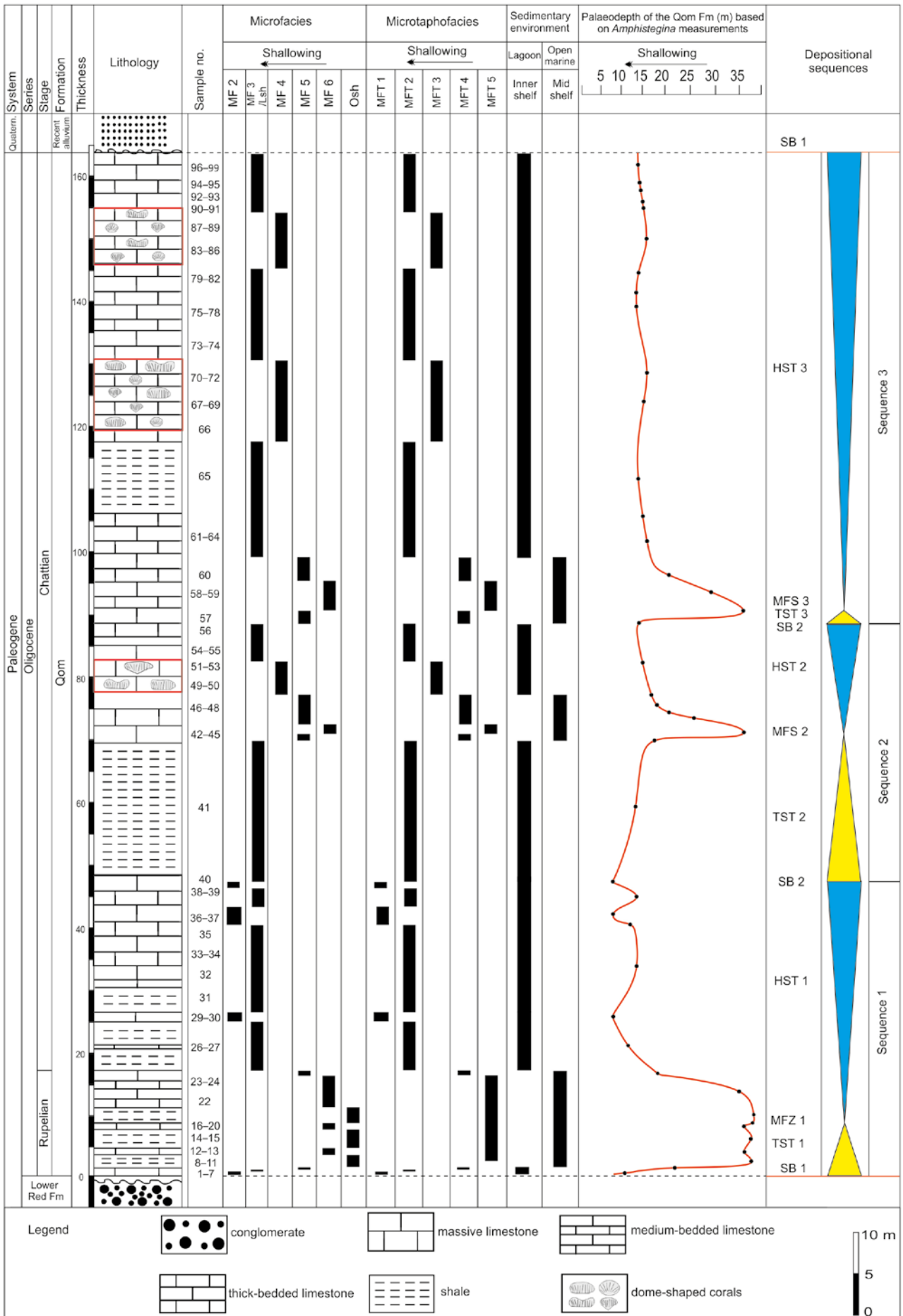
Fig. 6. Distribution chart of the microfacies and depositional sequences in the Abadeh section.
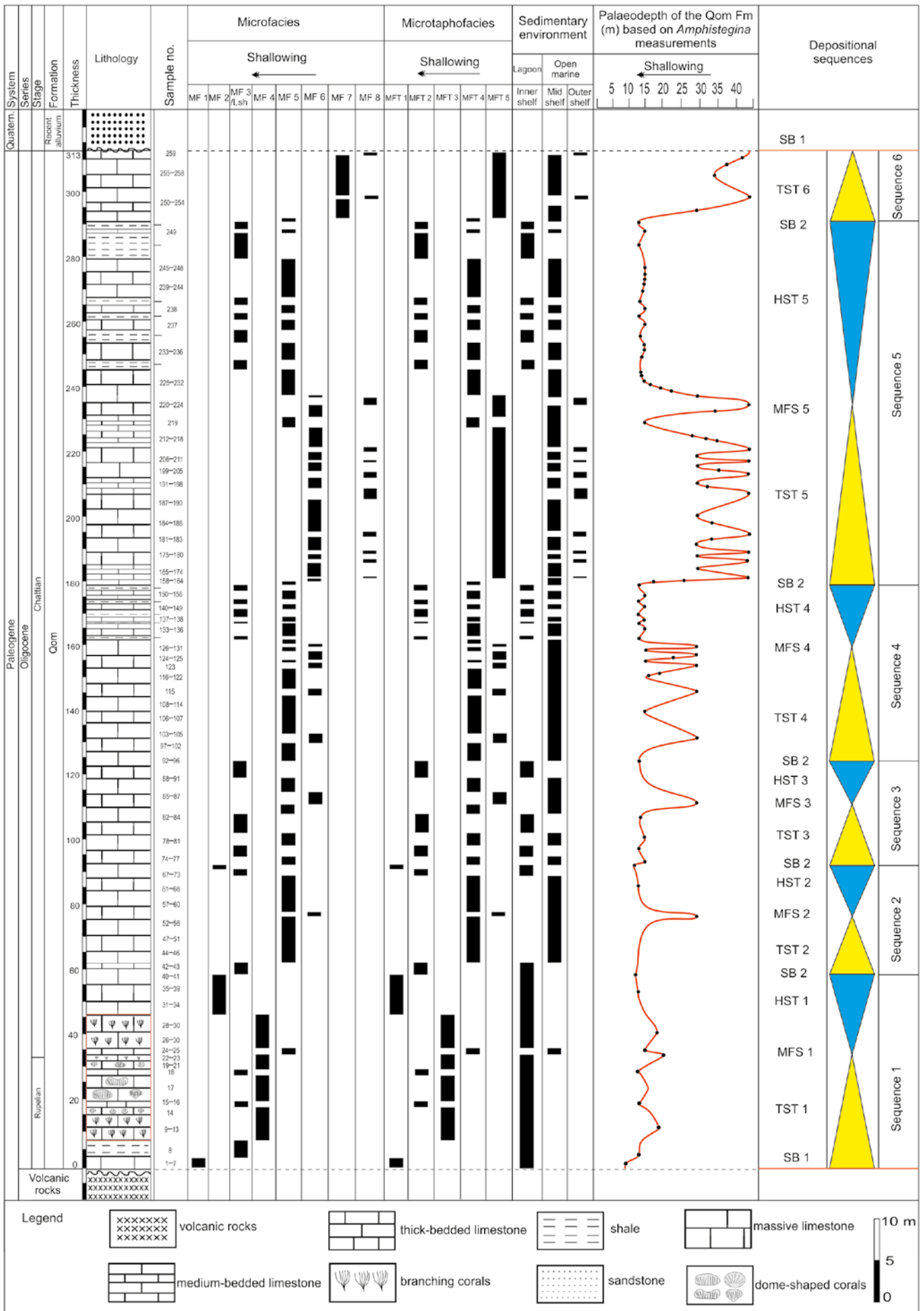
Fig. 7. Distribution chart of the microfacies and depositional sequences in the Ghamsar section.
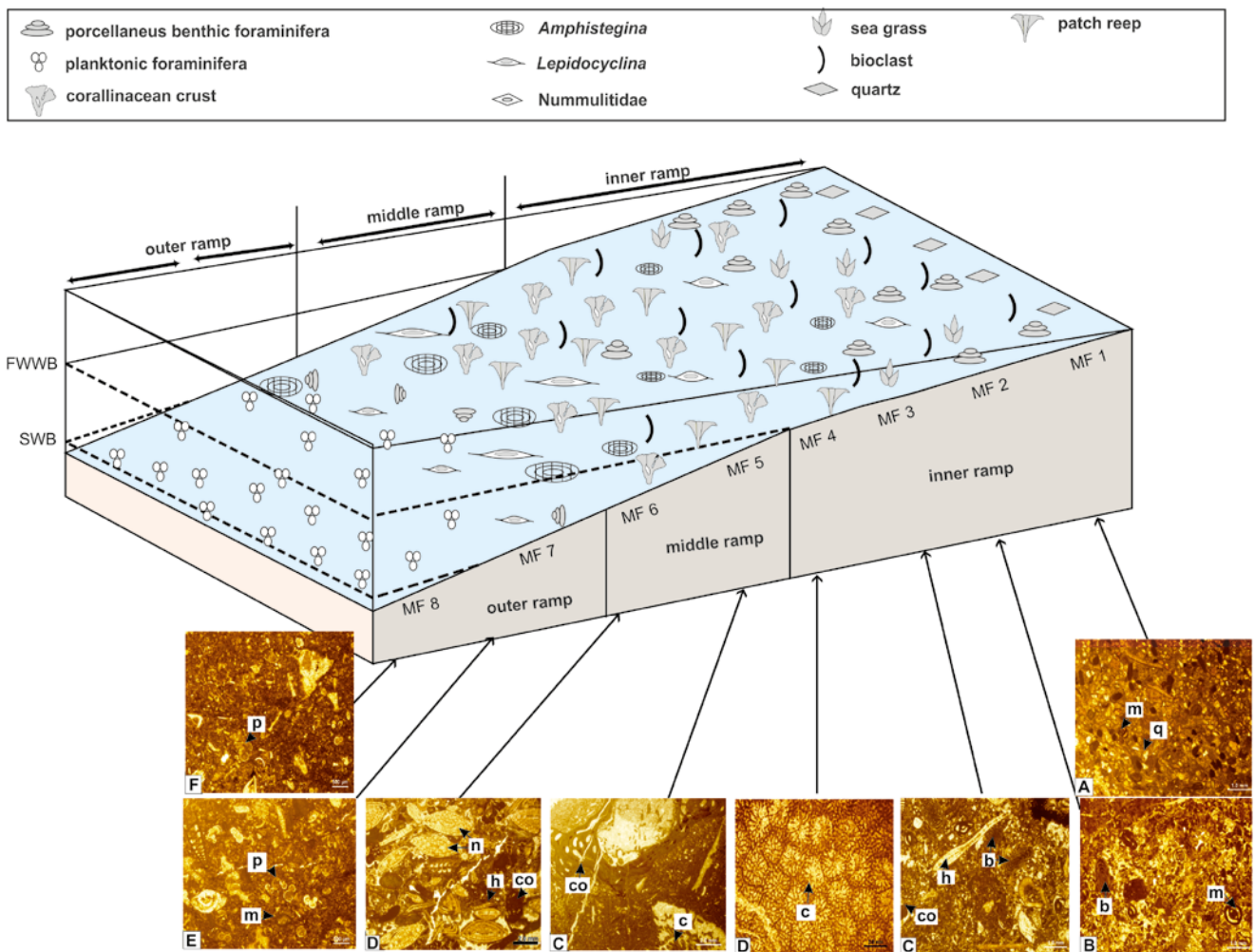
Fig. 8. Schematic model of the homoclinal carbonate ramp for depositional of the Qom Formation in the study sections (q – quartz grains; m – Miliolids; b – *Borelis*; h – *Heterostegina*; co – Corallinaceae; c – coral; n – *Nummulites*; p – planktonic foraminifera).

Therefore, the planktonic foraminifera bioclast packstone (MF 7) was formed in the outer ramp environment. The absence of large benthic foraminifera with planktonic foraminifera indicates sedimentation in the outer ramp environment with aphotic conditions as well as below the storm wave base (Geel, 2000; Ćosović *et al.*, 2004; Brandano *et al.*, 2016).

The bioclast planktonic foraminifera wackestone-packstone (MF 8) was deposited in the outer ramp environment. The main components of the fifth microtaphofacies in the Abadeh section are similar to those of MF 6 and in the Ghamsar section are similar to MFs 6, 7 and 8, formed in middle and outer ramp environments. The low rate of damage to the outer margin of a benthic foraminifera test (category 1) indicates transportation of the foraminifera test over short distances (Beavington-Penney, 2004). Considering the rates of taphonomic signatures as well as the higher fragmentation and transportation of benthic foraminifera tests (especially MF 7) in the Ghamsar section, it can be concluded that the fifth microtaphofacies in the Ghamsar section was deposited in a relatively higher-energy environment, compared to the Abadeh section.

Sequence stratigraphy

The definition of terminologies and conceptual models of sequence stratigraphy were presented by Sarg (1988), Van Wagoner *et al.* (1988), Wilgus *et al.* (1988) and Handford and Loucks (1993). The low-stand systems tract (LST), transgressive systems tract (TST), high-stand systems tract (HST), and falling-stage systems tract (FSST) were defined by Catuneanu *et al.* (2010, 2011). On the basis of sequence stratigraphy studies and the distribution of microfacies, five third-order sequences and one incomplete depositional sequence were identified in the Ghamsar section; and three third-order depositional sequences in the Abadeh section (Figs 6, 7, 9, 10).

Sequence 1

The sequence boundary between the Qom Formation and the Lower Red Formation in the Abadeh section, and the Qom Formation and the Eocene volcanic rocks in the Ghamsar section is a Type I sequence boundary (SB 1). It and one erosional surface (indicating exposure) are observed in both sections. The first sequence in the Ghamsar
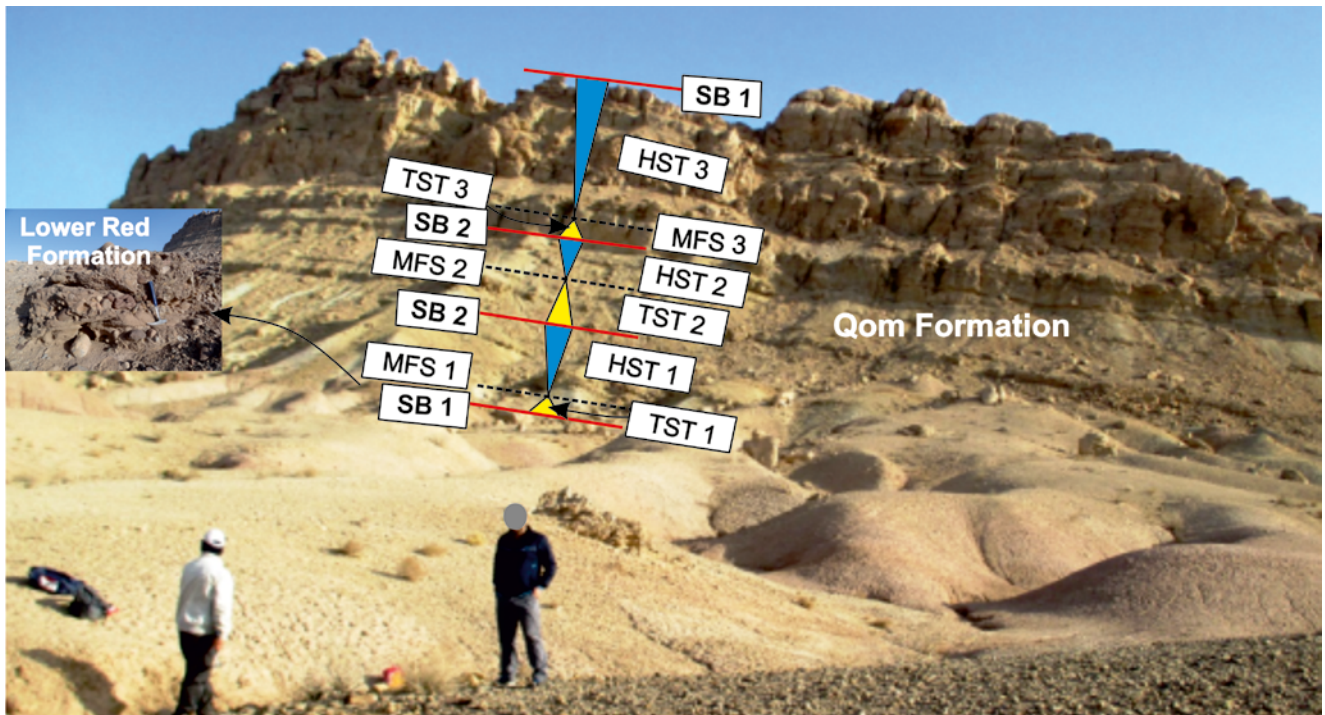
Fig. 9.   Outcrop photograph of the depositional sequences in the Abadeh section.

section (58.5 m) and the Abadeh section (47.5 m) consists of alternating shale and medium- and thick-bedded to massive limestone of Rupelian and Chattian ages (Figs 11, 12).

In both sections, the transgression begins with shallow-water microfacies. The TST in the Abadeh section includes 9 m of open-marine shale (shale facies – Osh) and inner (MFs 2, 3) and middle ramp (MFs 5, 6) limestones. Meanwhile, in the Ghamsar section, this systems tract (TST) with a thickness of 33.5 m included shallow-water shale (Lsh) and medium- and thick-bedded to massive limestones, belonging to a shallow-water environment (inner ramp; MFs 1, 3, 4). The maximum flooding surface (MFS) of this sequence in the Ghamsar section is marked by packstone-floatstone with bioclastic coral corallinaceae (MF 5). The Osh, belonging to an open marine environment and with a thickness of 3 m, represents the maximum flooding zone (MFZ) in the Abadeh section. In both sections, sedimentation of this depositional sequence continued during the Chattian Age. The medium-bedded limestones belonging to the middle ramp environment (MF 5) and massive limestones with scattered coral colonies and MFs 4 and 2 with a thickness of 25 m in HST were formed in the Ghamsar section. The HST, with a thickness of 38.5 m in the Abadeh section, included medium- to thick-bedded to massive limestones belonging to middle ramp environment (MFs 5, 6) and marine shallow water (MFs 2, 3). Bioclastic corallinaceae imperforate foraminifera packstone-grainstone (MF 2) indicates a type II sequence boundary (SB 2) between the first and second depositional sequences in both study sections. Evidence of exposure (such as an erosion surface) is absent at this sequence boundary in the study sections.

Sequence 2

The second depositional sequence in the Ghamsar section with a thickness of 33.5 m included thick-bedded to massive limestones (Fig. 12). This depositional sequence, with a thickness of 41 m, in the Abadeh section included shale and massive to thick-bedded limestones (Fig. 11). Transgression of the sea is reflected in the Ghamsar section by inner ramp limestones (bioclast corallinaceae imperforate and perforate foraminifera floatstone-packstone – MF 3) and in the Abadeh section by shallow-water shales (Lsh). In the Ghamsar section, a 17.5-m-thick TST consists of thick-bedded to massive limestones, belonging to the inner ramp environment (bioclast corallinaceae imperforate and perforate foraminifera floatstone-packstone – MF 3) and the middle ramp environment (bioclast coral corallinaceae packstone-floatstone – MF 5).

The TST with a thickness of 23.5 m consists of shallow-water shales and middle ramp limestones (bioclast coral corallinaceae packstone-floatstone) in the Abadeh section. The bioclastic corallinaceae perforate foraminifera packstone-floatstone (MF 6) indicates the MFS in both sections. The massive limestones, formed in the middle ramp environment (MFs 5, 6) and the inner ramp environment (MFs 2–4), belong to the HST in the Ghamsar and Abadeh sections. The bioclastic corallinaceae imperforate foraminifera packstone-grainstone (MF 2) in the Ghamsar section and bioclastic corallinaceae imperforate and perforate foraminifera floatstone-packstone (MF 3) in the Abadeh section indicate a sequence boundary of Type II between the second and third depositional sequences.
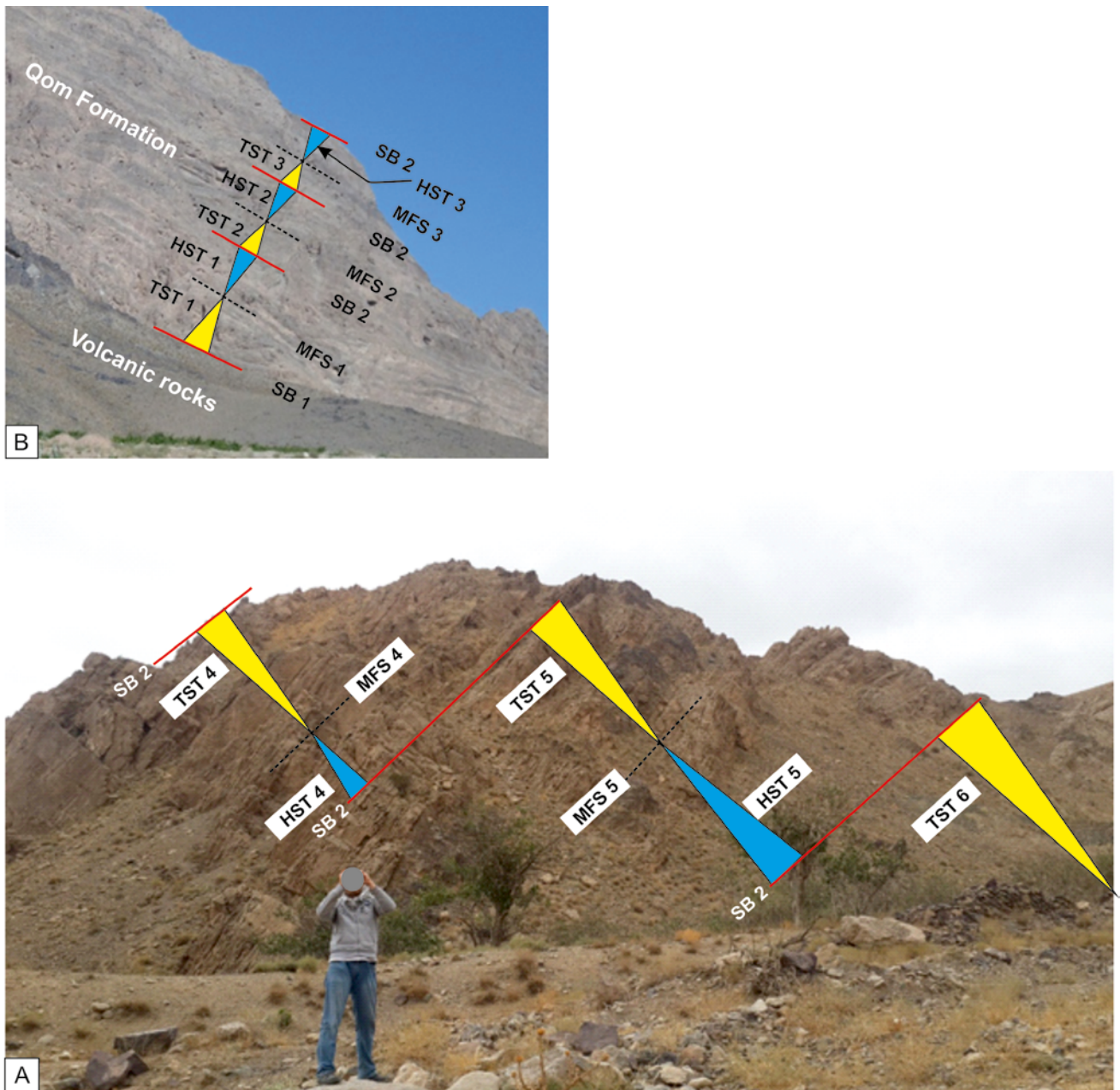
Fig. 10.   Field view photograph of the depositional sequences in the Ghamsar section (A, B).

Sequence 3

This depositional sequence, 32 m thick, is composed of medium- and thick-bedded limestones in the Ghamsar section (Fig. 12). The third depositional sequence in the Abadeh section consists of thick-bedded and massive limestones and shale with a thickness of 75.5 m (Fig. 13). The limestones belong to the inner ramp environment (bioclast corallinaceae imperforate and perforate foraminifera floatstone-packstone, MF 3) and middle ramp environment (bioclast coral corallinaceae packstone-floatstone, MF 5) with a thickness of 19 m were deposited in a TST.

Bioclastic coral corallinaceae packstone-floatstone (MF 5) was formed during the TST in the Abadeh section. The MFS in both study sections is determined by bioclastic corallinaceae perforate foraminifera packstone-floatstone (MF 6).

The HST in both study sections includes middle ramp limestones (MFs 5, 6) and inner ramp environment (MFs 3, 4) as well as shallow-water shales (Lsh). Bioclastic corallinaceae imperforate and perforate foraminifera floatstone-packstone (MF 3) represents the sequence boundary of type II in the Ghamsar section between the third and fourth depositional sequences. An erosional surface in the Ghamsar section at this sequence boundary was not observed in field observations. The sequence boundary between the third depositional sequence in the Abadeh section and the Recent alluvial sediments is a Type I sequence boundary and is marked by evidence of exposure (such as an erosion surface).
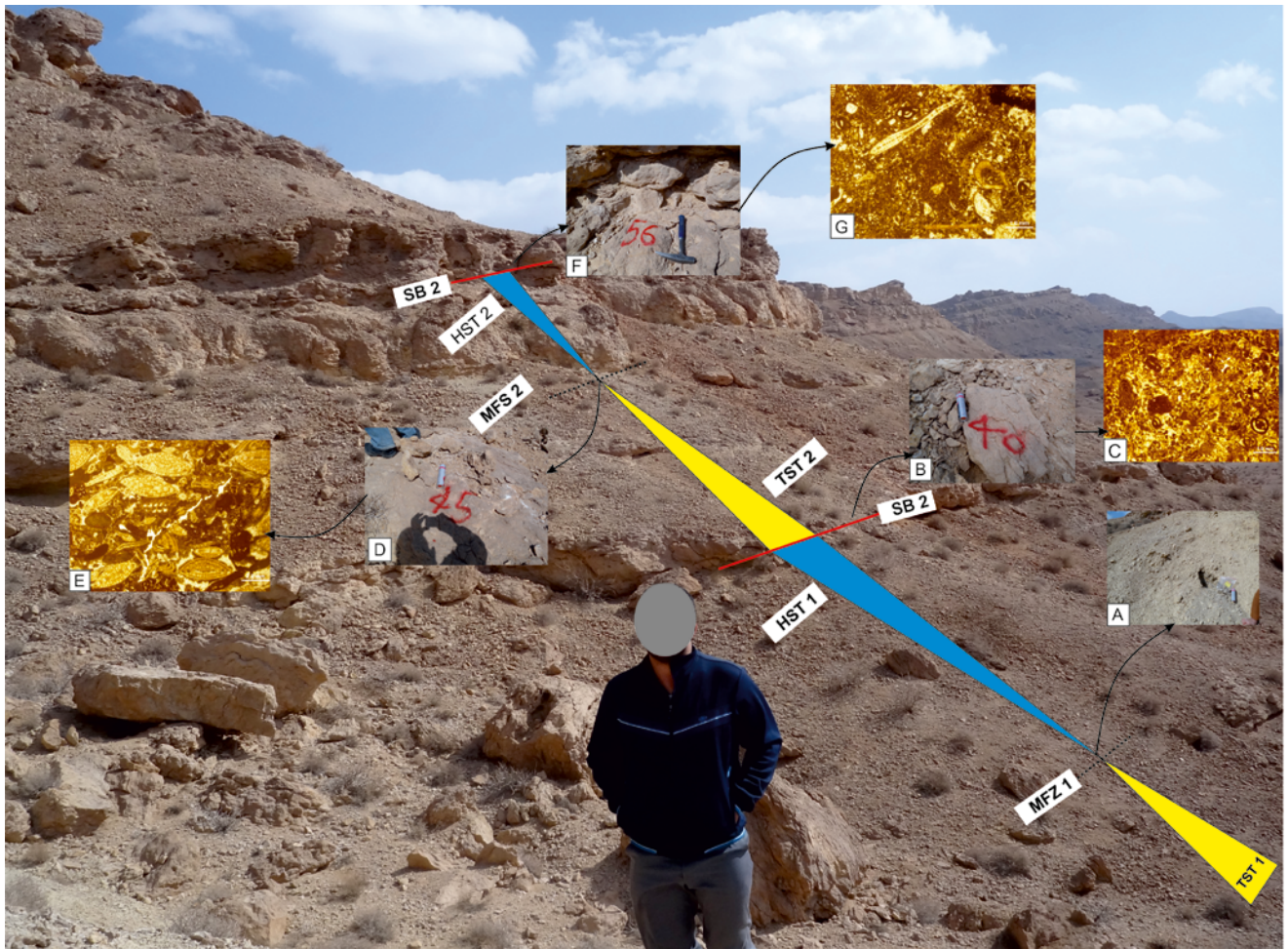
Fig. 11. Field picture of the first and second depositional sequences in the Abadeh section (TST, HST, MFS). **A.** General view of MFS 1. **B.** General view of sequence boundary. **C.** Sequence boundary in microscopic photograph (MF 2). **D.** General view of MFS 2. **E.** MFS 2 in microscopic photograph (MF 6). **F.** General view of sequence boundary. **G.** Sequence boundary in microscopic photograph (MF 3).
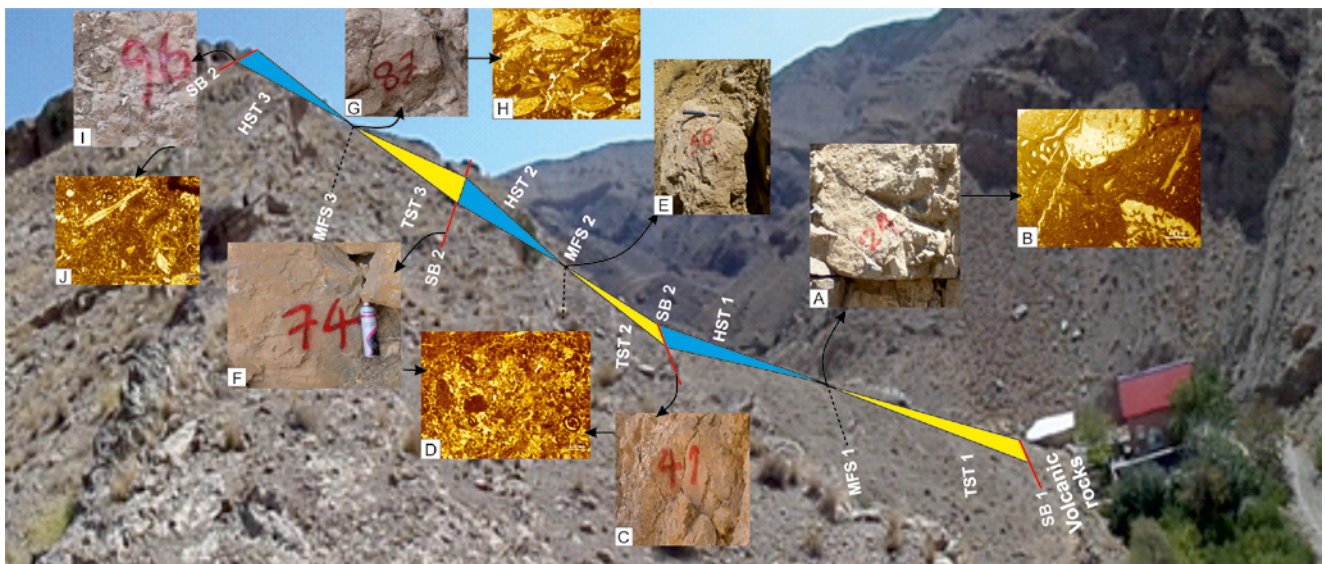
Fig. 12. Field picture of the first and second depositional sequences in the Abadeh section (TST, HST, MFS). **A.** General view of MFS 1. **B.** MFS 2 in microscopic photograph (MF 5). **C.** General view of sequence boundary. **D.** Sequence boundary in microscopic photograph (MF 2). **E.** MFS 2 in microscopic photograph (MF 6). **F.** General view of sequence boundary. **G.** General view of MFS 3. **H.** MFS 3 in microscopic photograph (MF 6). **I.** General view of sequence boundary. **J.** Sequence boundary in microscopic photograph (MF 3).
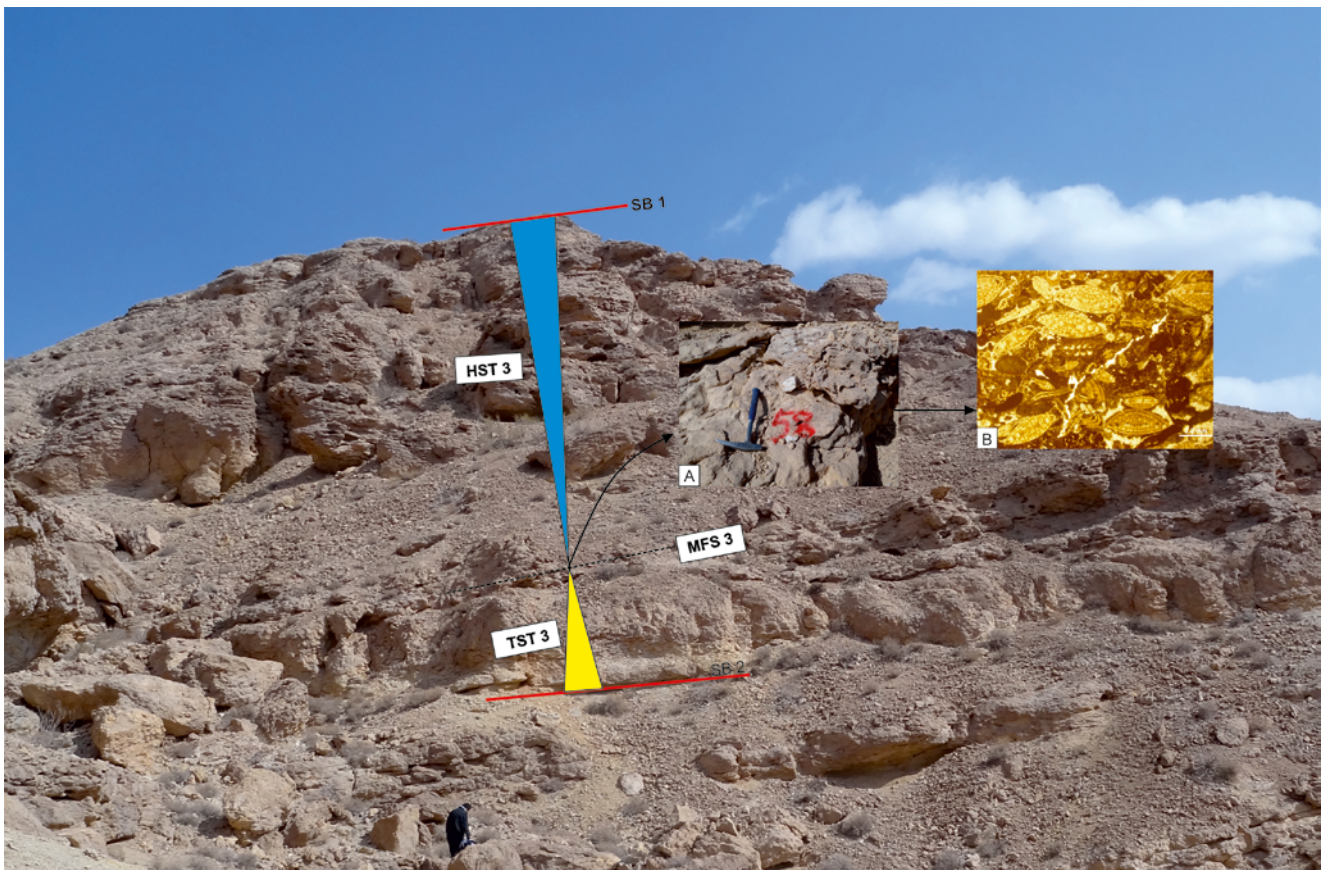
Fig. 13. Field picture of the third depositional sequences in the Abadeh section (TST, HST, MFS). **A.** General view of MFS 3. **B.** MFS 3 in microscopic photograph (MF 6).

Sequence 4

This depositional sequence, 55 m thick, in the Ghamsar section is composed of medium- and thick-bedded limestones and shales (Fig. 14). The thick-bedded limestones belong to the middle ramp environment (MFs 5, 6) and were deposited during the TST. Bioclastic corallinaceae perforate foraminifera packstone-floatstone (MF 6) represent the MFS. The HST consists of middle ramp limestones (MFs 5, 6) and shallow-water shales. The shallow-water shales (Lsh) represent the sequence boundary of Type II between the fourth and fifth depositional sequences and evidence of exposure (such as an erosion surface) was not observed in the study sections.

Sequence 5

This depositional sequence, 112 m thick, was observed only in the Ghamsar section (Fig. 15). The fifth depositional sequence consists of medium- and thick-bedded and massive limestone and shale. The TST with a thickness of 55 m consists of middle and outer ramp limestones (MFs 5, 6, 8). The MFS is characterized by bioclastic planktonic foraminifera wackestone-packstone (MF 8). The middle and outer ramp limestones (MFs 5, 6, 8), as well as 57-m-thick shallow-water shales (Lsh facies), represent the HST. The sequence boundary between the fifth and sixth depositional sequences is marked by shallow-water shales (Lsh). This sequence boundary is the sequence boundary of Type II without any evidence of exposure (such as an erosion surface).

Sequence 6

This incomplete depositional sequence was deposited in the Ghamsar section with a thickness of 22 m of massive limestones (Fig. 15). This depositional sequence includes only the TST, and MF 5, MF 7, and MF 8 were deposited during this systems tract. The sequence boundary between the Qom Formation and the Recent alluvial sediments is a Type I sequence boundary. Evidence of exposure, such as an erosion surface, can be seen in the field.

Correlation between depositional sequences in the Qom Sea sub-basins and the southern margin of Neotethys (Zagros Sea)

Bozorgnia (1966), Aghanabati (2006), Mohammadi *et al.* (2013) showed that a transgression happened from the southern margin of Neotethys (Zagros Sea) and from the southeast to the northwest of the central Iran zone. Local faults during the Oligocene-Miocene were active and influential in the Central Iran zone. Mahyad *et al.* (2019), Safari *et al.* (2020a, b) showed the influence of local faults on depositional sequences and the connection between the Qom back-arc sub-basin and Paratethys basin and stated that local faults were more effective than global sea-level changes and sea-level changes in the southern margin of the Zagros (Asmari Sea) and Paratethys basins on the formation of the depositional sequences of this sub-basin.
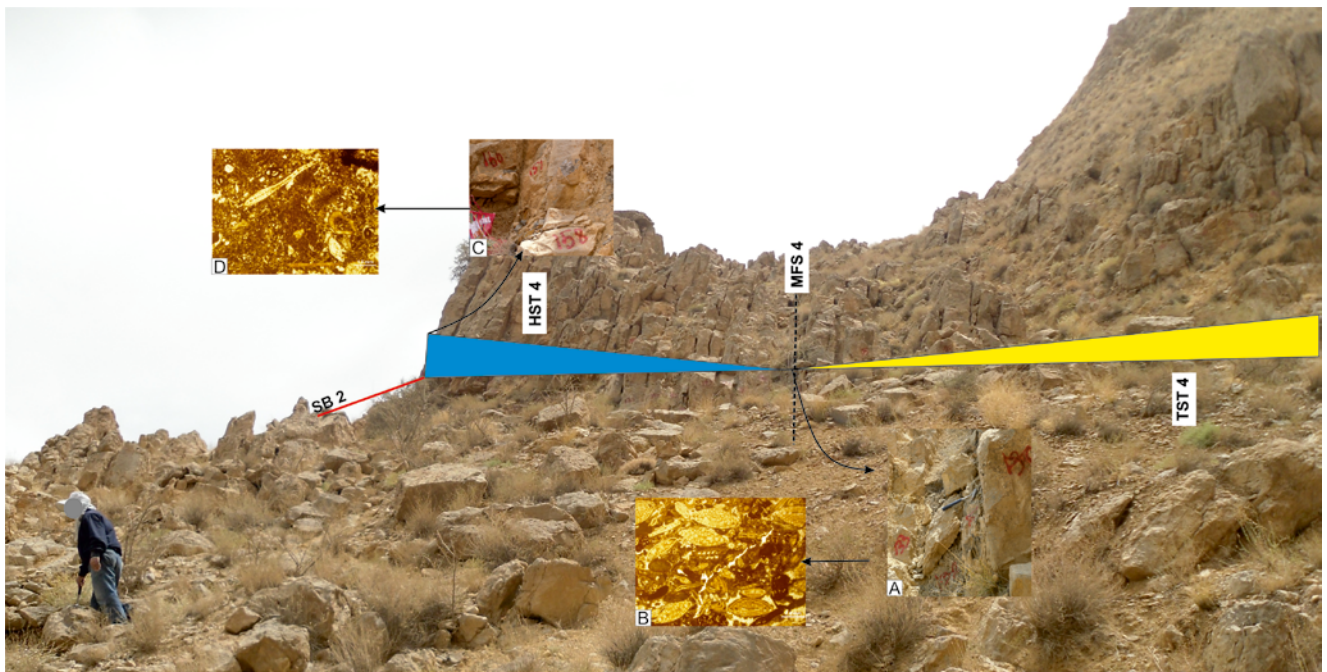
Fig. 14. Field picture of the fourth depositional sequences in the Ghamsar section (TST, HST, MFS). **A.** General view of MFS 4. **B.** MFS 3 in microscopic photograph (MF 6). **C.** General view of sequence boundary. **D.** Sequence boundary in microscopic photograph (MF 3).
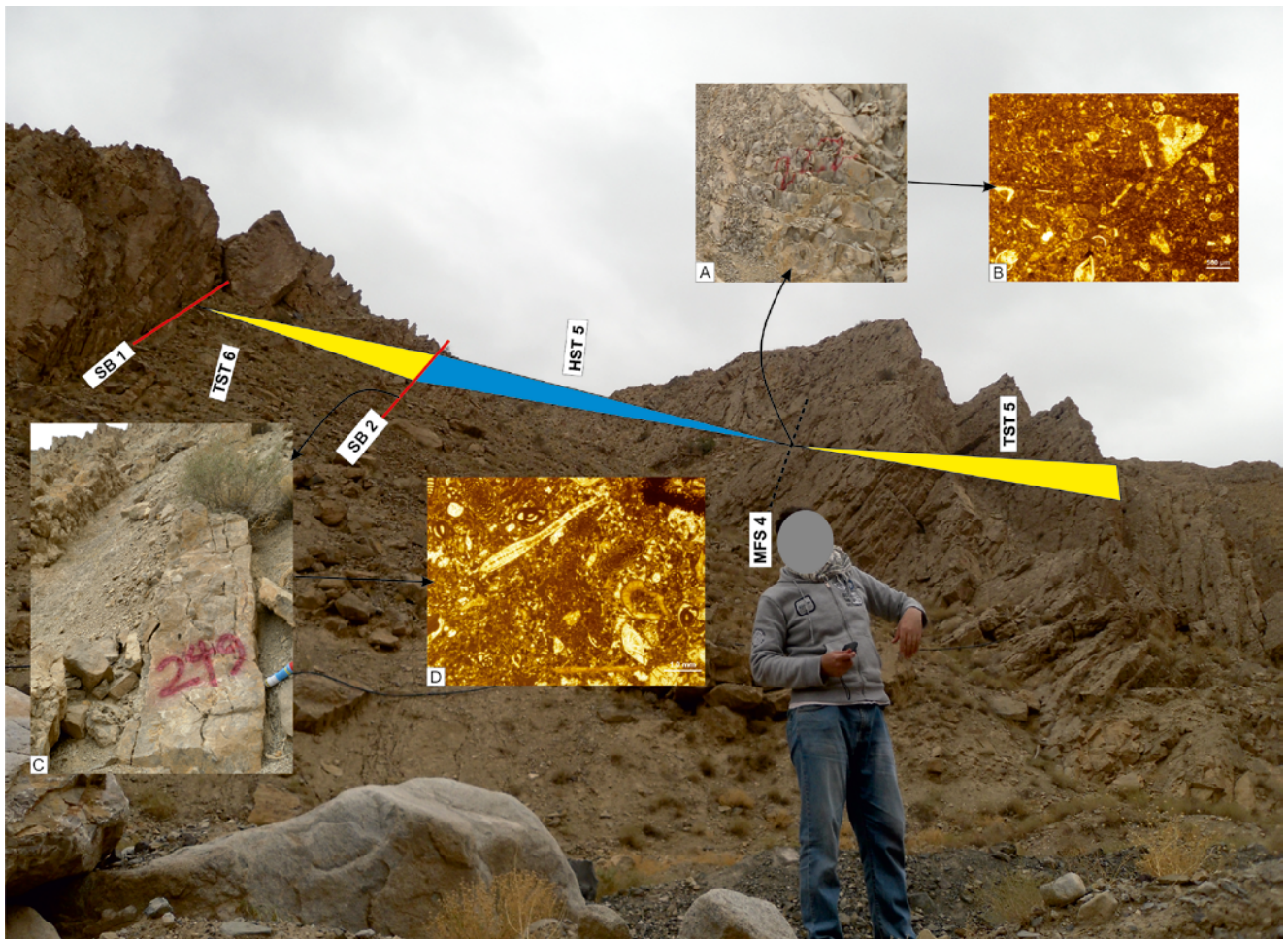
Fig. 15. Field picture of the fifth and sixth depositional sequences in the Ghamsar section (TST, HST, MFS). **A.** General view of MFS 5. **B.** MFS 5 in microscopic photograph (MF 8). **C.** General view of sequence boundary. **D.** Sequence boundary in microscopic photograph (MF 3).

However, the effect of these local faults on the depositional sequences of the Urumieh-Dokhtar arc and Esfahan-Sirjan fore-arc sub-basins have received less attention. For this purpose, the results of Vakarcs *et al.* (1998), Ehrenberg *et al.* (2007), van Buchem *et al.* (2010), Mahyad *et al.* (2019), Safari *et al.* (2020a, b) were used in this study. Correlation of the depositional sequences indicates that sea-level changes in the Paratethys basin and global sea-level changes had the least effect on the formation of depositional sequences in the Urumieh-Dokhtar arc and Esfahan-Sirjan fore-arc sub-basins (Fig. 16).

In addition, local faults have caused the number of depositional sequences formed in all three sedimentary sub-basins (fore-arc, magmatic arc and back-arc of Qom basin) to be different from each other. The changes in the number of depositional sequences indicate that sea-level changes in all three sedimentary sub-basins during the Chattian Age probably were independent. The correlation of depositional sequences shows that in all sedimentary sub-basins of the Qom Formation, the function and activity of local faults during the Chattian Age was more than in the Rupelian Age. This was while the function and effect of local faults on the number of depositional sequences in the Urumieh-Dokhtar arc sub-basin was higher than in other sedimentary sub-basins (Mahyad *et al.*, 2019; Safari *et al.*, 2020a, b). In addition, on the basis of correlation of depositional sequences,

it can be said that the effect of sea-level changes of Zagros Sea on the formation of depositional sequences in the Esfahan-Sirjan fore-arc sub-basin was significant (Vakarcs *et al.*, 1998; Ehrenberg *et al.*, 2007; Morley *et al.*, 2009; Van Buchem *et al.*, 2010).

CONCLUSIONS

Sedimentological and taphonomic studies led to the identification of eight carbonate microfacies, two terrigenous facies, and five microtaphofacies. The microfacies and microtaphofacies were deposited on a homoclinal carbonate ramp. This carbonate platform can be divided into inner, middle and outer ramp environments.

On the basis of the distribution of microfacies and sequence stratigraphy studies, five third-order depositional sequences and one incomplete depositional sequence were identified in the Ghamsar section; and three third-order depositional sequences in the Abadeh section. On the basis of the distribution of microtaphofacies, the energy, evidenced in the Ghamsar section was higher than that in the Abadeh section. In addition, the results of palaeobathymetric studies based on *Amphistegina* show that the Qom Formation in the Ghamsar section was formed in a deeper sea than that in the Abadeh section. The function of local faults was more
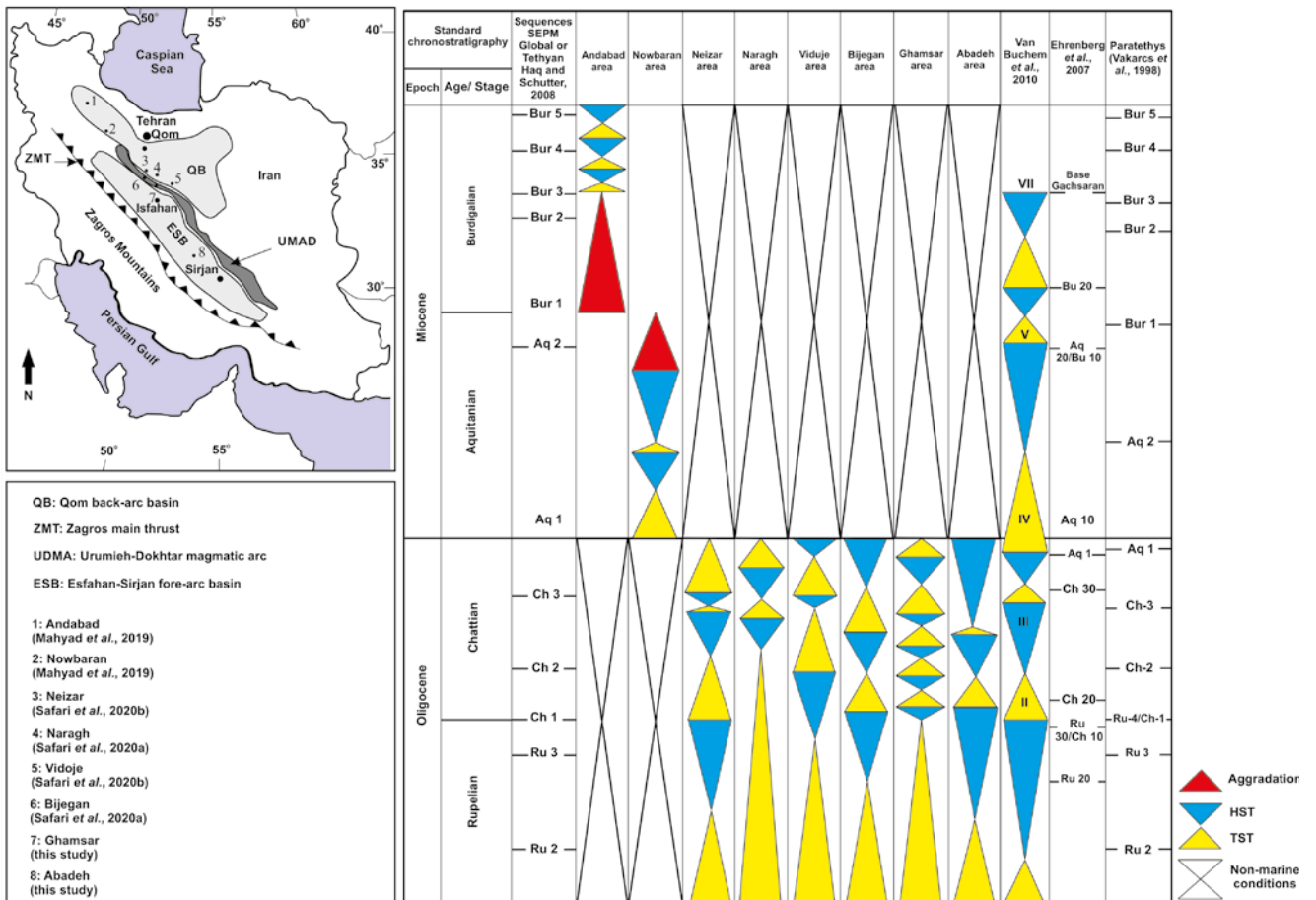
Fig. 16. Depositional sequences and palaeogeographical map. **A.** Palaeogeographical map of the Qom basin on the Iranian plateau (Schuster and Wielandt, 1999). **B.** Correlation of depositional sequences between the Qom Sea sub-basins and the Neotethys (Asmari sea) and Paratethys basins.

effective than sea-level changes in the Paratethys basin and global sea-level changes in the formation of depositional sequences in the Urumieh-Dokhtar arc and the Esfahan-Sirjan fore-arc sub-basins. The differences in the number of depositional sequences in the Qom back-arc, Urumieh-Dokhtar arc, and Esfahan-Sirjan fore-arc sub-basins can be related to the activity of local faults. The activity of local faults in all three sub-basins of the Qom Formation during the Chattian Age (especially within the Urumieh-Dokhtar arc sub basin) was more severe than during the Rupelian Age. The sea-level changes of the Zagros Sea were effective in the formation of depositional sequences in the Esfahan-Sirjan fore-arc sub-basin.

Acknowledgments

REFERENCES

Abaie, I. L., Ansari, H. J., Badakhshan, A. & Jaafari, A., 1964. History and development of the Alborz and Sarajeh fields of Central Iran. *Bulletin of Iranian Petroleum Institute*, 15: 561–574.

Afzal, J., Williams, M., Leng, M. J. & Aldridge, R. J., 2011. Dynamic response of the shallow marine benthic ecosystem to regional and pan-Tethyan environmental change at the Paleocene–Eocene boundary. *Palaeogeography, Palaeoclimatology, Palaeoecology,* 309: 141–160.

Aghanabati, A., 2006. *Geology of Iran*. Geological Survey of Iran, Tehran, 538 pp. [In Persian.]

Allison, P. A. & Bottjer, D. J., 2011. *Taphonomy: Process and Bias through Time*. Springer, New York, 603 pp.

Amidi, S. M. & Zahedi, M., 1991. *Geological Quadrangle Map of Iran no. F7 (Kashan), Scale 1:250 000*. Geological Survey of Iran.

Beavington-Penney, S. J., 2004. Analysis of the effects of abrasion on the test of *Palaeonummulites venosus*: implications for the origin of nummulithoclastic sediments. *Palaios*, 19: 143–155.

Beavington-Penney, S. J., Wright, V. P. & Racey, A., 2006. The middle Eocene Seeb Formation of Oman: an investigation of acyclicity, stratigraphic completeness, and accumulation rates in shallow marine carbonate settings. *Journal of Sedimentary Research*, 76: 1137–1161.

Berberian, M., 2005. The 2003 Bam urban earthquake: A predictable seismotectonic pattern along the western margin of the rigid Lut block, southeast Iran. *Earthquake Spectra*, 21: 35–99.

Berberian, M. & King, G. C. P., 1981. Towards a paleogeography and tectonic evolution of Iran. *Canadian Journal of Earth Sciences*, 18: 210–265.

Berning, B., Reuter, M., Piller, W. E., Harzhauser, M. & Kroh, A., 2009. Larger foraminifera as a substratum for encrusting bryozoans (Late Oligocene, Tethyan Seaway, Iran). *Facies*, 55: 227–241.

Bover-Arnal, T., Ferrandez-Canadell, C., Aguirre, J., Esteban, M., Fernandez-Carmona, J., Albert-Villanueva, E. & Salas, R., 2017. Late Chattian platform carbonates with benthic foraminifera and coralline algae from the SE Iberian plate. *Palaios*, 32: 61–82.

Bozorgnia, F., 1966. Qum formation stratigraphy of the Central Basin of Iran and its intercontinental position. *Bulletin of the Iranian Petroleum Institute*, 24: 69–76.

Brachert, T. C., Betzler, C., Braga, J. C. & Martin, J. M., 1998. Microtaphofacies of a warm-temperate carbonate ramp (uppermost Tortonian/lowermost Messinian, southern Spain). *Palaios*, 13: 459–475.

Brandano, M., Cornacchia, I., Raffi, I. & Tomassetti, L., 2016. The Oligocene–Miocene stratigraphic evolution of the Majella carbonate platform (Central Apennines, Italy). *Sedimentary Geology*, 333: 1–14.

Brandano, M., Frezza, V., Tomassetti, L. & Pedley, M., 2009. Facies analysis paleoenvironmental interpretation of the Late Oligocene Attard Member (Lower Coralline Limestone Formation), Malta. *Sedimentology*, 56: 1138–1158.

Brandano, M., Lipparini, L., Campagnoni, V. & Tomassetti, L., 2012. Downslope-migrating large dunes in the Chattian carbonate ramp of the Majella Mountains (Central Apennines, Italy). *Sedimentary Geology*, 255: 29–41.

Brandano, M., Morsilli, M., Vannucci, G., Parente, M., Bosellini, F. & Mateu-Vicens, G., 2010. Rhodolith-rich lithofacies of the Porto Badisco Calcarenites (upper Chattian, Salento, southern Italy). *Italian Journal of Geosciences*, 129: 119–131.

Buxton, M. W. N. & Pedley, H. M., 1989. A standardized model for Tethyan Tertiary carbonates ramps. *Journal of the Geological Society*, 146: 746–748.

Catuneanu, O., Bhattacharya, J. P., Blum, M. D., Dalrymple, R. W., Eriksson, P. G., Fielding, C. R., Fisher, W. L., Galloway, W. E., Gianolla, P., Gibling, M. R. & Giles, K. A., 2010. Sequence stratigraphy: common ground after three decades of development. *First Break*, 28: 41–54.

Catuneanu, O., Galloway, W. E., Kendall, C. G. S. C., Miall, A. D., Posamentier, H. W., Strasser, A. & Tucker, M. E., 2011. Sequence stratigraphy: methodology and nomenclature. *Newsletters on Stratigraphy*, 44: 173–245.

Ćosović, V., Drobne, K. & Moro, A., 2004. Palaeoenvironmental model for Eocene foraminiferal limestone of the Adriatic carbonate platform (Istrian Peninsula). *Facies*, 50: 61–75.

Ćosović, V., Drobne, K. & Ibrahimpašić, H., 2012. The role of taphonomic features in the palaeoecological interpretation of Eocene carbonates from the Adriatic carbonate platform (PgAdCP). *Neues Jahrbuch für Geologie und Paläontologie*, 265: 101–112.

Dunham, R. J., 1962. Classification of carbonate rocks according to depositional texture. In: Ham, W. E. (ed.), *Classification of Carbonate Rocks. American Association of Petroleum Geologists Memoir*, 1: 108–121.

Ehrenberg, S. N., Picard, N. A. H., Laursen, G. V., Monibi, S., Mossadegh, Z. K., Svana, T. A., Aqrawi, A. A. M., McArthur, J. M. & Thirlwall, M. F., 2007. Strontium isotope stratigraphy of the Asmari Formation (Oligocene–Lower Miocene), SW Iran. *Journal of Petroleum Geology*, 30: 107–128.

Embry, A. F. & Klovan, J. E., 1971. A Late Devonian reef tract on northeastern Banks Island, Northwest Territories. *Bulletin of Canadian Petroleum Geology*, 19: 730–781.

Flügel, E., 2010. *Microfacies of Carbonate Rocks, Analysis, Interpretation and Application*. Springer, Berlin, 984 pp.

Furrer, M. A. & Soder, P. A., 1955. The Oligo-Miocene Marine Formation in the Qum Region (Iran). In: *Proceedings of the Fourth World Petroleum Congress, Rome, Section I/A/5.* Carlo Colombo Publisher in Rome, pp. 267–277.

Gansser, A., 1955. New aspects of the geology in Central Iran. In: *Proceeding of the Fourth World Petroleum Congress, Rome, Section I/A/5.* Carlo Colombo Publisher in Rome, pp. 279–300.

Geel, T., 2000. Recognition of stratigraphic sequence in carbonate platform and slope deposits: empirical models based on microfacies analysis of Paleogene deposits in southeastern Spain. *Palaeogeography, Palaeoclimatology, Palaeoecology*, 155: 211–238.

Greenstein, B. J. & Pandolfi, J. M., 2003. Taphonomic alteration of reef corals: Effects of reef environment and coral growth form II: The Florida Keys. *Palaios*, 18: 495–509.

Halfar, J., Godinez-Orta, L., Mutti, M., Valdez-Holguín, J. E. & Borges, J. M., 2004. Nutrient and temperature controls on modern carbonate production: an example from the Gulf of California, Mexico. *Geology*, 32: 213–216.

Hallock, P., 1999. Symbiont-bearing foraminifera. In: Gupta, B. K. S. (ed.), *Modern Foraminifera*. Kluwer, Dordrecht, pp. 123–139.

Hallock, P. & Glenn, E. C., 1986. Numerical analysis of foraminiferal assemblages: A tool for recognizing depositional facies in Lower Miocene reef complexes. *Journal of Paleontology*, 59: 1382–1394.

Hallock, P. & Hansen, H. J., 1979. Depth adaptation in *Amphistegina*: change in lamellar thickness. *Bulletin of the Geological Society of Denmark*, 27: 99–104.

Handford, C. R. & Loucks, R. G., 1993. Carbonate depositional sequences and systems tracts-responses of carbonate platforms to relative sea level changes. In: Loucks, R. G. & Sarg, J. F. (eds), *Carbonate Sequence Stratigraphy – Recent Developments and Applications. American Association of Petroleum Geologists Memoir,* 57: 3–41.

Harzhauser, M. & Piller, W. E., 2007. Benchmark data of a changing sea-palaeogeography, palaeobiogeography and events in the Central Paratethys during the Miocene. *Palaeogeography, Palaeoclimatology, Palaeoecology*, 253: 8–31.

Heydari, E., 2008. Tectonics versus eustatic control on supersequences of the Zagros Mountains of Iran. *Tectonophysics*, 451: 56–70.

Heydari E., Hassanzadeh, J., Wade, W. J. & Ghazi, A. M., 2003. Permian–Triassic boundary interval in the Abadeh section of Iran with implications for mass extinction. Part 1 – sedimentology. *Palaeogeography, Palaeoclimatology, Palaeoecology*, 193: 405–423.

Hottinger, L., 2000. Functional morphology of benthic foraminiferal shells, envelopes of cells beyond measure. *Micropaleontology*, 46: 57–86.

Knoerich A. C. & Mutti, M., 2003. Controls of facies and sediment composition on the diagenetic pathway of shallow water heterozoan carbonates: The Oligocene of the Maitese Islands. *International Journal of Earth Sciences*, 92: 494–510.

Langer, M. R. & Hottinger, L., 2000. Biogeography of selected "larger" foraminifera. *Micropaleontology*, 46: 105–126.

Larsen, A. R. & Drooger, C. W., 1977. Relative thickness of the test in the *Amphistegina* species of the Gulf of Elat. *Utrecht Micropaleontological Bulletins*, 15: 225–239.

Mahyad, M., Safari, A., Vaziri-Moghaddam, H. & Seyrafian, A., 2019. Biofacies, taphofacies, and depositional environments in the north of Neotethys Seaway (Qom Formation, Miocene, Central Iran). *Russian Geology and Geophysics*, 60: 1368–1384.

Mateu-Vicens, G., Hallock, P. & Brandano, M., 2009. A depositional model and paleoecological reconstruction of the Lower Tortonian distally steepened ramp of Menorca. *Palaios*, 23: 465–481.

Mohammadi, E. & Ameri, H., 2015. Biotic components and biostratigraphy of the Qom Formation in northern Abadeh, Sanandaj–Sirjan fore-arc basin, Iran (northeastern margin of the Tethyan Seaway). *Arabian Journal of Geosciences*, 8: 10789–10802.

Mohammadi, E., Hasanzadeh-Dastgerdi, M., Ghaedi, M., Dehghan, R., Safari, A., Vaziri-Moghaddam, H., Baizidi, C., Vaziri, M. R. & Sfidari, E., 2013. The Tethyan Seaway Iranian Plate Oligo-Miocene deposits (the Qom Formation): distribution of Rupelian (Early Oligocene) and evaporate deposits as evidences for timing and trending of opening and closure of the Tethyan Seaway. *Carbonates and Evaporites*, 28: 321–345.

Mohammadi, E., Safari, A., Vaziri-Moghaddam, H., Vaziri, M. R. & Ghaedi, M., 2011. Microfacies analysis and paleoenvironmental interpretation of the Qom Formation, south of the Kashan, Central Iran. *Carbonates Evaporites,* 26: 255–271.

Morley, C. K., Kongwung, B., Julapour, A. A., Abdolghafourian, M., Hajian, M., Waples, D., Warren, J., Otterdoom, H., Srisuriyon, K. & Kazemi, H., 2009. Structural development of a major late Cenozoic basin and transpressional belt in central Iran: the Central Basin in the Qom-Saveh area. *Geosphere*, 4: 325–362.

Nadimi, A., 2007. Evolution of the Central Iranian basement. *Gondwana Research*, 12: 324–333.

Nebelsick, J. H. & Bassi, D., 2000. Diversity, growth forms and taphonomy: key factors controlling the fabric of coralline algae dominated shelf carbonates. *Geological Society, London, Special Publications*, 178: 89–107.

Nebelsick, J. H., Bassi, D. & Lempp, J., 2013. Tracking paleoenvironmental changes in coralline algal-dominated carbonates of the Lower Oligocene Calcareniti di Castelgomberto formation (Monti Berici, Italy). *Facies*, 59: 133–148.

Nebelsick, J. H., Bassi, D. & Rasser, M. W., 2011. Microtaphofacies: Exploring the potential for taphonomic analysis in carbonates. In: Allison, P. A. & Bottjer, D. J. (eds), *Taphonomy. Aims and Scope Topics in Geobiology Book, Series.* Springer, Dordrecht, pp. 337–373.

Payros, A., Pujalte, V., Tosquella J. & Orue-Etxebarria, X., 2010. The Eocene storm-dominated foralgal ramp of the western Pyrenees (Urbasa-Andia Formation): An analogue of future shallow-marine carbonate systems. *Sedimentary Geology*, 228: 184–204.

Perry, C. T., 2005. Structure and development of detrital reef deposits in turbid nearshore environments, Inhaca Island, Mozambique. *Marine Geology*, 214: 143–161.

Pomar, L., 2001. Type of carbonate platform: A genetic approach. *Basin Research*, 13: 313–334.

Pomar, L., Baceta, J. I., Hallock, P., Mateu-Vicens, G. & Basso, D., 2017. Reef building and carbonate production modes in the west-central Tethys during the Cenozoic. *Marine and Petroleum Geology*, 83: 261–304.

Pomar, L., Mateu-Vicens, G., Morsilli, M. & Brandano, M., 2014. Carbonate ramp evolution during the Late Oligocene (Chattian), Salento Peninsula, southern Italy. *Palaeogeography, Palaeoclimatology, Palaeoecology*, 404: 109–132.

Quaranta, F., Tomassetti, L., Vannucci, G. & Brandano, M., 2012. Coralline algae as environmental indicators: a case study from the Attard Member (Chattian, Malta). *Geodiversitas*, 34: 151–166.

Read, J. F., 1982. Carbonate platforms of passive (extensional) continental margins-types, characteristics and evolution. *Tectonophysics*, 81: 195–212.

Read, J. F., 1985. Carbonate platform facies models. *Geological Society of America Bulletin*, 69: 1–21.

Reuter, M., Piller, W. E., Harzhauser. M., Mandic, O., Berning, B., Rögl, F., Kroh, A., Aubry, M. P., Wielandt-Schuster, U. & Hamedani, A., 2009. The Oligo-/Miocene Qom Formation (Iran): evidence for an early Burdigalian restriction of the Tethyan Seaway and closure of its Iranian gateways. *International Journal of Earth Sciences*, 98: 627–650.

Romero, J., Caus. E. & Rosell, J., 2002. A model for the palaeoenvironmental distribution of larger foraminifera based on late Middle Eocene deposits on the margin of the South Pyrenean basin (NE Spain). *Palaeogeography, Palaeoclimatology, Palaeoecology*, 179: 43–56.

Safari, A., Ghanbarloo, H., Kasiri, A. & Purnajjari, S. M., 2020b. Sedimentary environment and depositional sequences of the Oligocene Qom Formation in Central Iran based on micro-facies and microtaphofacies analysis. *Carbonates and Evaporites*, 35: 1–22.

Safari, A., Ghanbarloo, H., Mansoury, P. & Esfahani, M. M., 2020a. Reconstruction of the depositional sedimentary environment of Oligocene deposits (Qom Formation) in the Qom Basin (northern Tethyan seaway), Iran. *Geologos*, 26: 93–111.

Sarg, J. F., 1988. Carbonate sequence stratigraphy. In: Wilgus, C. K., Hastings, B. S., Kendall, C. G. St. C., Posamentier, H. W., Ross, C. A. & Van Wagoner, J. C. (eds), *Sea-Level Changes: An Integrated Approach. Society for Sedimentary Geology, Special Publication*, 43: 155–181.

Sarkar, S., 2017. Microfacies analysis of larger benthic foraminifera-dominated Middle Eocene carbonates: a palaeoenvironmental case study from Meghalaya, NE India (Eastern Tethys). *Arabian Journal of Geosciences*, 5: 1–13.

Schuster, F. & Wielandt, U., 1999. Oligocene and Early Miocene coral faunas from Iran: palaeoecology and palaeobiogeography, *International Journal of Earth Sciences*, 88: 571–581.

Silvestri, G., Bosellini, F. R. & Nebelsick, J. H., 2011. Microtaphofacies analysis of lower Oligocene turbid-water coral assemblages. *Palaios*, 26: 805–820.

Stocklin, J. & Setudehnia, A., 1991. Stratigraphic Lexicon of Iran. *Geological Survey of Iran Publication*, *Report*, 18: 1–376.

Taraz, H. & Aghanabati, A., 1993. *Geological Quadrangle Map of Abadeh, Scale 1:250 000*. Geological Survey of Iran.

Vakarcs, G., Hardenbol, J., Abreu, V. S., Vail, P. R., Várnai, P. & Tari, G., 1998. Oligocene-Middle Miocene depositional sequences of the central Paratethys and their correlation with regional stages. *SEPM Special Publication*, 60: 209–231.

Van Buchem, F. S. P., Allan, T. L., Laursen, G. V., Lotfpour, M., Moallemi, A., Monibi, S., Motiei, H., Pickard, N. A. H., Tahmasbi, A. R., Vedrenne, V. & Vincent, B., 2010. Regional stratigraphic architecture and reservoir types of the Oligo-Miocene deposits in the Dezful Embayment (Asmari and Pabdeh Formations), SW Iran. *Geological Society Special Publications*, 32: 219–263.

Van Wagoner, J. C., Posamentier, H. W., Mitchum, R. M., Vail, P. R., Sarg, J. F., Loutit, T. S. & Hardenbol, J., 1988. An overview of the fundamentals of sequence stratigraphy and key definitions. In: Wilgus, C. K., Hastings, B. S., Kendall, C. G. St. C., Posamentier, H. W., Ross, C. A. & Van Wagoner, J. C. (eds), *Sea-Level Changes: An Integrated Approach. Society for Sedimentary Geology, Special Publication,* 42: 38–45.

Wilgus, C. K., Hastings, B. S., Posamentier, H., Wagoner, T. V., Ross, C. A. & Kendall, C. G., 1988. Sea level changes: an integrated approach. *Society for Sedimentary Geology*, *Special Publication*, 42: 1–407.

Yazdi, M., Shirazi, M. P., Rahiminejad, A. H. & Motavalipoor, R., 2012. Paleobathymetry and paleoecology of colonial corals from the Oligocene–early Miocene (?) Qom Formation (Dizlu area, central Iran). *Carbonates and Evaporites*, 27: 395–405.